Spring 1960

SORPTION AND DIFFUSION IN POLYVINYL ACETATE AND OTHER LINEAR AMORPHOUS POLYMERS

ROGER PEABODY KAMBOUR

Mic 60-4454

KAMBOUR, Roger Peabody. SORPTION AND DIFFUSION IN POLYVINYL ACETATE AND OTHER LINEAR AMORPHOUS POLYMERS.

University of New Hampshire
Ph.D., 1960
Chemistry, physical

University Microfilms, Inc., Ann Arbor, Michigan

SORPTION AND DIFFUSION IN POLYVINYL ACETATE AND OTHER LINEAR AMORPHOUS POLYMERS

BY

ROGER PEABODY BARRER

B.A., Amherst College, 1954

A THESIS

Submitted to the University of New Hampshire

In Partial Fulfillment of

The Requirements for the Degree of

Doctor of Philosophy

Graduate School

Department of Chemistry

June, 1960

This thesis has been examined and approved.

Frank L. Pilar

Alexander R. Emlen

May 21, 1960
Date

ACKNOWLEDGMENT

This work was carried out under the patient and understanding guidance of Dr. Frank L. Pilar to whom the author is indebted for his constant encouragement and many stimulating discussions.

Support of the project was provided in part by a grant from the Central University Research Fund which is gratefully acknowledged.

This thesis is dedicated to the author's wife, Virginia D. Kambour, whose support in all things was vital to the completion of this work.

TABLE OF CONTENTS

LIST OF TABLES

FIGURES

DEFINITIONS OF SYMBOLS

Symbol	Definition
C	Temperature constant in Sutherland's eq.
c	Diffusant concentration
CE	Molar cohesion energy
CED	Cohesive energy density
CSA_c	Collision cross-sectional area of diffusion molecule
CSA_p	Molecular cross-sectional area from the parachor
D	True diffusion coefficient
$\bar{D}$	Integral diffusion coefficient
D_o	Limiting diffusion coefficient at zero vapor concentration
d	Density
d_1	Density of diffusant in liquid state
d_2	Density of dry polymer
d_e	Liquid density
d_v	Vapor density
$\Delta E^{\ddagger}$	Diffusion activation energy
$\Delta E_2^{\ddagger}$, $\Delta E_1^{\ddagger}$	Activation energies above and below T_g respectively
e	Naperian logarithm base
e_1, e_2	Cohesive energies per gram
$\Delta F^{\ddagger}$	Diffusion activation free energy
$\Delta \bar{F}_1^{*}$	$-T \Delta \bar{S}_1^{*}$
$\Delta \bar{F}_{1n}$	Non-ideal relative partial molal free energy of the vapor in solution
f	Number of activated degrees of freedom in the diffusion zone

Definition of Symbols (cont.)

Symbol	Definition
ΔH_v	Heat of vaporization
$\Delta \bar{H}_{1n}$	Relative partial molal enthalpy of the vapor
h	Planck's constant
K	Initial slope of normalized weight pickup vs $t^{1/2}$
K_s	K for sorption
K_d	K for desorption
k	Boltzmann constant
L	Hole length in unit diffusion step
l	Film thickness
M	Molecular weight
N	Avogadro's number
N_1, N_2	Mole fractions
P	Parachor
P_i	Internal pressure
P/P_o	Relative vapor pressure
$\bar{r}$	Average molecule radius at $0^{\circ}K$
R	Gas constant
$\Delta S^{\ddagger}$	Diffusion activation entropy
$\Delta \bar{S}_1^*$	Ideal relative partial molal entropy of the vapor
$\Delta \bar{S}_{1n}$	Non-ideal relative partial molal entropy of the vapor in solution
ΔS_v	Entropy of vaporization
T	Temperature
T_g	Glass transition temperature

Definition of Symbols (cont.)

Symbol	Definition
t	Time
V	Volume fraction of component in solution
V_f	Free volume fraction
V_M	Molar volume
V_v	Volume of one mole of vapor under its own vapor pressure
$\Delta V^{\ddagger}$	Activation volume
$\Delta V_2^{\ddagger}, \Delta V_1^{\ddagger}$	Activation vols. above and below T_g respectively
v	Specific volume
v_f	Free volume
v_o	Molecular volume at $0^{\circ}K$
W, W_∞	Equilibrium weight of sorbed vapor per unit weight of polymer
W_t	Weight of sorbed vapor per unit weight of polymer at time t
x	Distance from film surface
χ	Number of polymer chain segments per molecule
α	Slope of ln $\bar{D}$ vs concentration of sorbed vapor (page 7)
α	Coefficients of cubical thermal expansion (page 84)
α_1	Coefficients of Instantaneous thermal expansion
α_2	Coefficients of equilibrium thermal expansion
α_W	Slope of ln $\bar{D}$ vs W line
α_V	Slope of ln $\bar{D}$ vs V_1 line
β	Isothermal compressibility

Definition of Symbols (cont.)

Symbol	Definition
γ	Surface tension
λ	Diffusion path length
σ_T	Molecular collision diameter at temperature T
σ_∞	Molecular collision diameter at infinite temperature
χ_1	Flory-Huggins parameter of the vapor

INTRODUCTION

I. INTRODUCTION

Purpose

The work reported herein was initiated as the beginning of a long-range series of studies in this laboratory of permeation and diffusion in polymer films in both the dry and plasticized states. The first objective was the obtaining of equilibrium isotherms of a number of organic vapors in polyvinyl acetate for the purpose of extending studies of gas permeation and diffusion in polymer films containing known concentrations of organic vapor. The second was the obtaining of sorption-desorption kinetic data for the elucidation of the mechanisms of the diffusion of the organic vapors themselves in polyvinyl acetate.

Background

The phenomena of solubility, diffusion, and permeation of gases and vapors in high polymers constitute an area of research which has expanded considerably in the last two decades, largely as a result, of course, of the expanded commercial use of these materials. The significance of these studies, from an industrial viewpoint, is, among other things, related to plasticization, dye infusion, and to the use of polymer films as protective devices. The early studies were primarily concerned with rubbers and cellulosics, reflecting their earlier advent and widespread use, compared to the more recent plastic materials and synthetic fibers.

The last fifteen years, however, have seen the growth of a considerable amount of such studies utilizing a number of synthetic high polymers the molecular chains of which, in contrast to those of rubbers, can be considered completely linear. This class can be divided into two parts; the first consists of completely amorphous, linear polymers, the second contains those linear polymers which are partially crystalline. Polymers of styrene, vinyl acetate, the various acrylate and methacrylate esters are examples of the first type while certain polyethylenes, and polyethylene terephthalate exemplify the second.[1] This thesis is primarily concerned with the first type.

General Characteristics of Diffusion in Linear Amorphous High Polymers. Early investigations of sorption and diffusion phenomena in linear amorphous polymers brought out a number of salient features common to the class.

First, in contrast to the diffusion of the permanent gases, such as oxygen or hydrogen, in these media, the diffusion of organic vapors appeared to be markedly concentration dependent, the diffusion coefficient, D, increasing rapidly with concentration of organic impurity in the polymer.[2,3] Second, diffusion coefficients for the organic diffusants were found to be much lower than those for the permanent gases.

Third, diffusion properties of organic vapors into and through the polymers were found to differ greatly above and below the glass transition temperature, Tg, for the polymer.[4,5] The glass transition temperature is that point or

temperature range where the amorphous polymer properties change from those of a highly viscous liquid to those of a glass as temperature decreases. On a molecular level, this change is thought to correspond to the "freezing out" of motions large enough to allow the polymer to readjust, when a change in a thermodynamic variable such as temperature or composition occurs to a state of minimum free energy in a "short" period of time.[6] Above the glass transition temperature the diffusion coefficients of organic vapors in amorphous linear polymers are dependent only on concentration; below it they are time-dependent as well.[4] Whereas the former behavior can be accommodated by Fick's Law of Diffusion and is thus termed Fickian diffusion, the latter cannot and is correspondingly termed non-Fickian.

Measurement of Diffusion Coefficients

Traditionally diffusion coefficients of gases and vapors through solids have been determined by means of measurements of the fluxes of the diffusants through membranes of the solid materials as functions of time.[6] When a gas-membrane system is in a state of constant pressure drop across the membrane and constant gas flow through the membrane, measurements of these two quantities plus film thickness suffice to determine the permeability coefficient. When a gas-membrane system is initially in the steady state and the pressure differential is suddenly changed, measurements of this change, the time lag before the rate of effluence

changes, plus the membrane thickness, serve to determine the diffusion coefficient. Since the permeability coefficient is the product of the diffusion and solubility coefficients, these two types of experiment, with the same experimental apparatus often are thus enough to determine both diffusivities and solubilities. Such is true when the diffusion coefficient D is concentration dependent, but not when it is a function of time, since then the time lag measurements yield erroneous results.[7]

Another method of determining diffusivities and solubilities for vapors involves measurements of the absorption of vapor by films or slices of the solid suspended in a vapor medium as functions of time and vapor pressure, the equilibrium amount absorbed giving the solubility coefficient and the rate of attainment of this amount relating to the diffusion coefficient.[2-5] When diffusion coefficients are time-dependent, a combination of the steady state permeability measurements and the equilibrium absorption measurements are required to yield "true" diffusion coefficients.

Crank and coworkers in the late forties,[2,8] recognizing the convenient features of the sorption method of studying vapor diffusion, were able to develop methods for calculation of diffusion coefficients from rate-of-sorption experiments where diffusion was concentration dependent.

In cases where D is independent of concentration, Fick's Second Law of Diffusion[4,9]

$$\partial c/\partial t = \partial (D \partial c/\partial x) /\partial x \qquad (1)$$

can be simplified to

$$dc/dt = D\, d^2c/dx^2 \qquad (2)$$

where C is concentration of diffusant in the film, t is time and x is distance from the film surface. For sorption into a film of thickness l the boundary conditions for (2) are

$$c(0,t) = c(\ell,t) = c_f$$
$$c(x,0) = c_i \text{ for } -\ell/2 < x < \ell/2 \qquad (3)$$

where c_i and c_f are initial and final diffusant concentrations in the film.[4,9] These are equivalent to assuming that equilibrium of the diffusant at the film surface is attained instantaneously when the diffusant partial pressure at the film surface is changed, but at the instant of this change no change in concentration occurs anywhere inside the film. Under these conditions it can be shown that the absorption-time curve obtained when the diffusant pressure is suddenly increased by a certain increment coincides with the desorption-time curve obtained when the pressure is dropped by the same amount.[8] The diffusion coefficient is given[4] by

$$D = (\pi/16)K^2 = (\pi/16)\,(\Delta W_t/\Delta W)_\infty/t^{1/2} \qquad (4)$$

Here K is the slope of the initial straight line obtained by plotting the normalized weight change per unit film thickness against the square root of time. This equation holds until the concentration at the film center has begun to change.

When diffusion is concentration-dependent the sorption and desorption curves obtained as described above do not coin-

cide.[4,8] Furthermore the slope of the sorption or desorption-square root of time plot, although still initially constant, depends on the initial and final vapor concentrations. Crank and coworkers[8] were able to show that, from a series of pairs of sorption-desorption time curves, all lower concentrations being zero, but with increasing upper concentrations, true diffusion coefficients and their concentration dependences could be calculated. In brief it was found that the average of the apparent diffusion coefficient calculated from the sorption-time curve and that calculated from the corresponding desorption-time curve was related quite closely to the true diffusion coefficient at the upper concentration. The average apparent or so-called integral diffusion coefficient, $\bar{D}$, was found to be given by

$$\bar{D} = 1/c \int_{c=0}^{c} D\,dc \qquad (5)$$

where D is the true diffusion coefficient at the concentration C. That is, the integral diffusion coefficient is the appropriate average of the true diffusion coefficients over the particular concentration interval involved.

Although several methods of calculating $\bar{D}$ from the sorption-desorption curves exist, the procedure used in the experimental work on which part of this dissertation is based employs the following modification of (4), attributable to Long.[4]

$$\bar{D} = (\pi/32)\,(K_s^{\,2} + K_d^{\,2}) \qquad (6)$$

Here K_s and K_d are the slopes of the sorption and desorption

lines respectively.

Subsequent investigations have shown that diffusivities of organic vapors in polymeric films are always increasing functions of concentration,[2-5,10,11] at least when no chemical reaction between film and vapor occurs. In this situation, it is mathematically predictable as well as experimentally observable that K_s is larger than K_d.[4] In addition it is found experimentally that the integral diffusion coefficient can be related to concentration, in low concentration ranges by[3,4,10]

$$\bar{D} = D_0 e^{\alpha c} \qquad (7)$$

where α and D_0 are constants characteristic of the vapor-polymer pair. D_0 is the limiting diffusion coefficient as concentration approaches zero. It should be noted that no bar is placed over D_0 since

$$\lim_{c \to 0} \bar{D} = D_0$$

Finally combination of (5) and (7) yields[4]

$$D = D_0 (1 + \alpha c) e^{\alpha c} \qquad (8)$$

EXPERIMENTAL

II. EXPERIMENTAL

Sorption Apparatus

Equilibrium isotherms and sorption kinetic data were obtained utilizing fine quartz spiral springs (McBain balances) suspended in columns as shown in Figure 1. (As a result of the extremely slow rates of equilibrium attainment, e.g. ten days, found in an exploratory run with ethyl bromide at 25°, three sets of glass apparatus were built and housed in the same thermostat so that three sets of data could be obtained simultaneously. This addition was later proved somewhat unnecessary by the great increase in speed attendant with a rise in ambient temperature to 30°.) The sample of polyvinyl acetate was hung from the hook on the end of the spring by means of fine copper wire or a drawn glass or quartz fiber. One of the three springs used was assembled from the two parts of a spring which had been used and broken in the laboratory at some previous time, in the following way. Each coil was suspended by the hook, extended, and the last spiral at the broken end slipped over a knife blade to provide support and thermal isolation of the remainder of the coil. Using metal hooks and rods and a small, relatively cool, oxygen-gas flame it was possible to refashion the last spiral into a hook. The two repaired sections were then suspended one from the other to provide a completely adequate balance. This method of repair proved successful a number of times after breakage of springs.

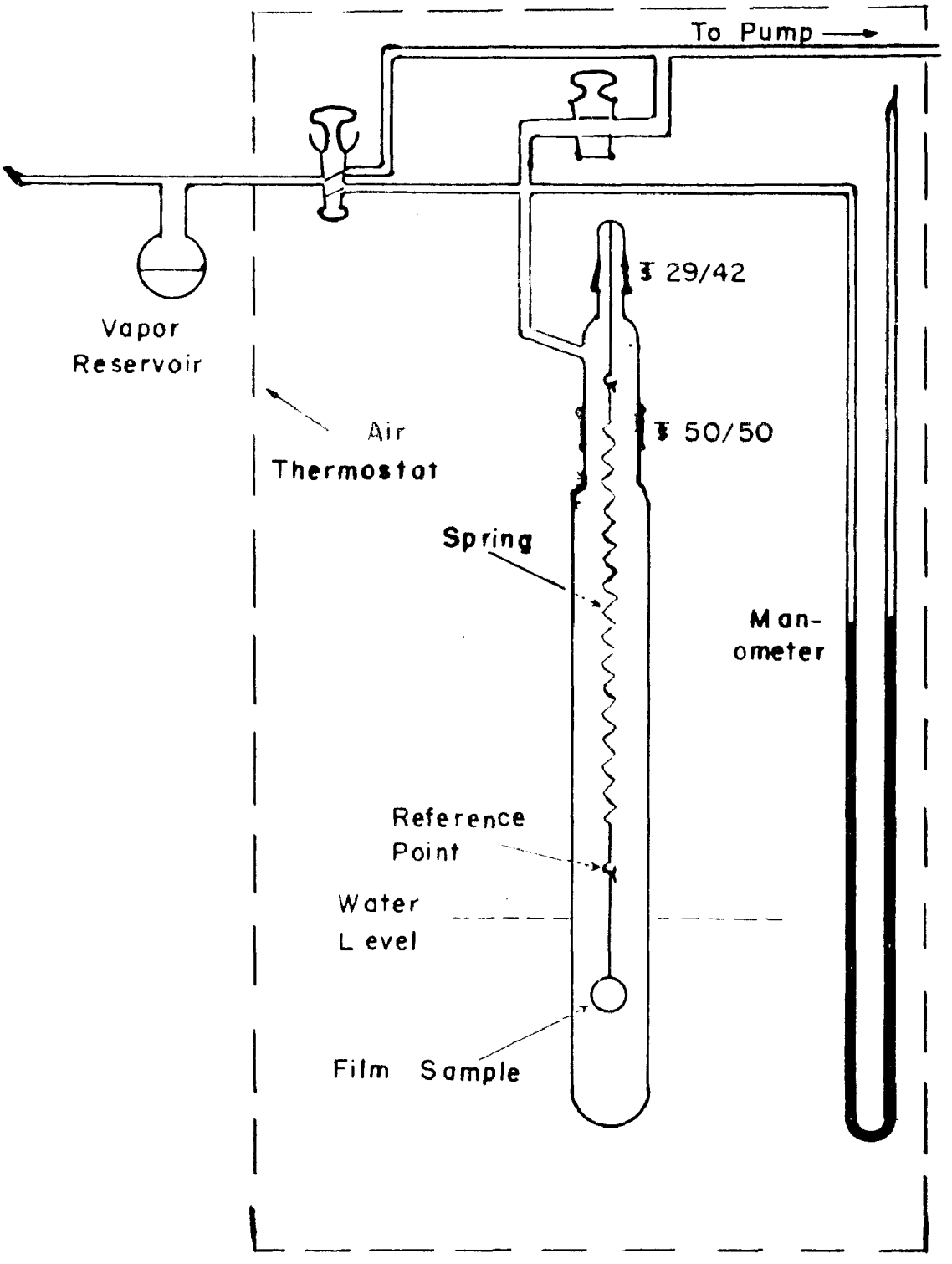

FIGURE 1 APPARATUS

The second and third springs used were obtained from Microchemical Specialties Company, Berkeley, California and had a capacity of 50 milligrams plus a safety margin of another 50 milligrams.

Calibration was effected by measuring extensions with a cathetometer when the spring was loaded with weighed pieces of wire. Sensitivities ranged from about 4.0 to 4.5 millimeters per milligram and could be determined to within a root mean square error of less than 1%. The Gaertner cathetometer used could be read to $\pm$ 0.05 millimeters corresponding to weights of 1×10^{-5} grams.

The spring was suspended in a 4 inch diameter glass column from the ground glass jointed cap. A second, larger joint was located a few inches below the cap joint. This arrangement of two joints seemed the one most convenient in terms of ease of changing the height of the spring support hook, and suspending or removing film samples and springs safely. Fear of setting up strains in the large section, which was more difficult to fabricate, caused the placement of the inlet connection in the upper section of the column, which was small enough to be annealed in a muffle furnace. This placement required that the inlet tube be cut every time the column was opened to change film samples.

A mercury manometer and stopcocks leading to the vapor reservoir and vacuum line were connected to the column inlet. The vacuum line stopcock was a wide bore one to enable the fastest possible column evacuation (see page 31). The stopcock on the vapor reservoir line was of the mercury seal

variety. Prior to sealing off the dead-end side of the manometer, both sides were evacuated and the air driven out of the mercury by heating it to boiling in small sections of the manometer at a time.

Apiezon greases were used to seal the stopcocks, the particular grease used depending on the temperature of operation. Apiezon wax, instead of grease, was used to seal the column's 50/50 joint, by application at the exposed edge only. This change was necessitated by the difficulty of opening this joint when greased and after being under vacuum for long periods of time. Moderate heat sufficed to melt the wax and to allow the joint to be opened.

A water bath of the required dimensions was built from sheet brass and mounted in an insulated box built specially for the purpose. A flat copper cooling coil was placed on the bottom of the bath. The water temperature was controlled with a Techne MK 111 Tempunit to $\pm$ 0.1 $^{\circ}$C. The lower end of the column was suspended in the bath. Its height, that of the spring suspension hook and the length of sample extension fibre or wire were adjusted so that the polymer sample hung several centimeters below the water bath level but the lower spring hook remained far enough above the top of the water bath to be used as the extension reference mark.

An air thermostat was built to encompass the water bath, column, manometer and all stopcocks. This consisted of a light wood frame in two sections covered with transparent plastic. Double glassed-in doors made up the front side.

The sections were easily removable for repair work,etc. Glass was used instead of plastic in the doors since through these observations of spring height were made. Temperature was controlled with a mercury-relay regulator, mercury expansion switch, heater, and fan to $\pm$ 1° C. of the water bath temperature. The thermostat enclosed the whole glass system except the vapor reservoir bulb. The addition of the air thermostat was necessitated by the discovery that when the room temperature (and thus that of the vapor in the upper part of the column) was below the bath temperature the resultant vapor layer inversion in the column was sufficiently unstable to produce convection currents strong enough to cool the sample temperature, thus changing the amount and rate of sorption. Such currents were sometimes strong enough to jiggle the sample and spring up and down, making spring extension readings very inaccurate.

Vapor Source Preparation

The ethyl bromide and acetonitrile used were from Matheson, Coleman, and Bell with boiling points 38-40° and 80-82° respectively.

Purification was accomplished by drying and fractional distillation of the liquids in the following manner. Sealed to the vapor reservoir bulb was a second bulb containing previously ignited calcium oxide to be used as a dessicant. The liquid was introduced, cooled to -78° C, and the opening sealed off under vacuum. The bulb was warmed to room temperature and the liquid dried for several hours. The first third of

the liquid was pumped off and the middle third allowed to distill over to the vapor reservoir by cooling it. Both bulbs were then cooled to -78°C and the connection between them sealed off under evacuation. The cooling and evacuation during glass sealing operations were necessary to prevent the accumulation of thermal degradation products of the vapor in the vapor reservoir. (Decomposition of ethyl bromide, for instance, yields hydrogen bromide, among other things, which chemisorbs in polyvinyl acetate.)

The vapor reservoir was situated outside the air thermostat so that its temperature could be independently and easily controlled.

Film Preparation

The polyvinyl acetate used was Vinac B-100 from the Colton Chemical Division of the Air Reduction Co. The viscosity average molecular weight was estimated to be 1-2 x 10^5.[12] The glass-transition for this molecular weight occurs at about 28-30°C.

Film samples were prepared by the technique of casting on a mercury surface which yields clear, homogeneous, strain-free films of even and controlled thicknesses.[6] Dry acetone was used to prepare solutions of the polymer of about 7 grams per liter. These were filtered to remove slight traces of insoluble particles. Chemically-cleaned and once-distilled mercury was poured into a petri dish in a dessicator and a clean steel ring of diameter slightly less than that of the dish laid on the mercury surface. Polymer solution in

the amount required to form a film of the desired thickness was pipetted onto the surface inside the ring. Evaporation of the solution was effected by air drying or by passage of dry nitrogen through the dessicator, depending on the relative humidity of the room. (When the acetone solution is wet the cast films have no strength).

After the film had formed, the ring was lifted from the mercury surface and placed in an atmosphere saturated with water vapor for at least 1 day in order to leach the film of residual acetone. (The water vapor essentially plasticized the film thereby increasing the rate of desorption of the large acetone molecule). The film, still on the steel ring, was then vacuum dried at temperatures up to 60-70 °C for about one week to remove the water vapor. Leaching prior to vacuum drying decreases the time required for the latter by as much as a month.[4,6] After drying the films were stored in dessicators.

Film sections of known area were cut from the rings in a dry box and weighed. From the weight, area, and the density of the polyvinyl acetate (determined here to be 1.16 grams per cubic centimeter) the film thickness was calculated.

It was found that the vapors used, even at low partial pressures, plasticized the films enough to cause their collapse when unsupported, making diffusion measurements impossible and increasing the times required for film-vapor equilibrium. Support was provided by threading through each film sample around its edge a length of 38 gauge copper wire to form a loop or ring strong enough to prevent film collapse

and yet light enough for the McBain balance. This procedure was a satisfactory one in terms of the film area stabilization but a very delicate, time-consuming and frustrating one in that the film had to be handled with tweezers throughout the operation, the wire had poor compressive strength and thus made a bad "needle", and the film had little tear strength once a hole was formed. A much better procedure was finally evolved; this consisted of forming the requisite loop of wire beforehand, weighing it, and then laying it in the evaporating acetone solution in the steel ring. The resultant film contained the loop completely imbedded in it. Fortunately amalgamation of the copper wire by the mercury surface did not occur. The leaching, drying and cutting processes were carried out as before, the weight of the sample being corrected for the wire loop.

Procedure

The film sample to be used was hung on the spring in the column, the system sealed up and evacuated until the spring extension was constant, and the system leak-tested.

The desired quantity of vapor was admitted by carefully controlled opening of the stopcock. (Too rapid admission caused the sample to bounce off the hook, the spring to bounce off its support, or even caused the spring spirals to become entangled amoung themselves. At the same time, it was desirable that vapor admission be rapid compared to the sorption half time, so that the boundary condition

DISCUSSION OF EXPERIMENTAL RESULTS

$c(0,t) = c(l,t) = c_f$ (cf. eqn. 3) obtained at zero time. Spring extension was then measured as a function of time after vapor admission with a stopwatch or clock, depending on sorption rates, until equilibrium obtained.

The equilibrium spring extension and the partial pressure were determined. (The volume of the column was large enough so that sorption by the sample resulted in negligible change in the partial pressure.)

The system was then evacuated as rapidly as possible and spring extension versus time again determined. Desorption was followed until the original spring extension obtained.

III. DISCUSSION OF EXPERIMENTAL RESULTS

Equilibrium Isotherms

Ideal behavior and the Flory Huggins Parameter.

Ideal behavior for dilute solutions of vapors or gases in polyvinyl acetate is considered here to involve a) obedience to Henry's Law, b) zero heat of mixing, and c) zero non-ideal entropy of mixing. The first and second criteria are self-explanatory; the third needs expansion.

For the solution of two low molecular weight substances the ideal, or statistical, entropy of mixing is given[1] by $-R\ (N_1 \ln N_1 + N_2 \ln N_2)$ where N is the mole fraction of the particular component. Because of the high molecular weight, the entropy of solution of polymers never approaches this quantity and the following expression offers closer approximation to the statistical entropies of polymer solution.[1]

$$\Delta \bar{S}_1^{*} = -R\ \ln(1-V_2) + (1-1/\chi)V_2 \qquad (9)$$

Here $\Delta \bar{S}_1^{*}$ is the relative partial molal configurational entropy of solvent in solution, V_2 is the volume fraction of polymer in solution, and χ is the number of polymer chain segments, of size equal to the solvent molecule size, in the polymer molecule. For high polymers $1/\chi$ is negligible.

The sum of the relative partial molal free energy of the solvent $\Delta \bar{F}_1$, and $T\Delta \bar{S}_1^{*}$ will then be a measure of what will be termed the non-ideal relative partial molal free

energy of the solvent $\Delta \bar{F}_{1n}$. Using P/P_o the partial pressure of the solvent, as its activity the following obtains from standard thermodynamic treatment,

$$\ln(P/P_o) = -\Delta\bar{F}_1/RT = -\Delta\bar{F}_{1n}/RT + \Delta\bar{S}_1^*/R$$
$$= -\Delta\bar{F}_{1n}/RT - \ln(1-V_2) + V_2 \qquad (10)$$

The Flory-Huggins treatment[1] defines a characteristic parameter χ_1 by

$$\Delta\bar{F}_{1n} = RT\,\chi_1\,V_2^2 \qquad (11)$$

This quantity may contain an enthalpy and/or an entropy term. Determination of χ_1 as a function of temperature serves to fix values of ΔH_{1n} the relative partial molal enthalpy of the solvent in solution, and thus by difference, the values of the non-ideal relative partial molal entropy. (Since any non-zero enthalpy indicates a non-ideal solution the subscript n on $\Delta\bar{H}_{1n}$ is superfluous. It has been retained for emphasis however.) A more direct test of the presence or absence of a heat of mixing comes from the comparison of the sorption isotherms at different temperatures since from (10)

$$(\ln P/P_o)/\,(1/T)_{V_2,P_T} = -\Delta\bar{H}_{1n}/R \qquad (12)$$

where P_T is the total pressure on the system.

Although a number of systems have been reported[13] wherein $\Delta\bar{H}_{1n}$ equals zero, none appears to have been found for which the non-ideal relative partial molal entropy $\Delta\bar{S}_{1n}$ is zero throughout an extensive range of concentration. Flory attributes this to failure of the model for the statistical entropy calculations and to the possible existence of

local ordering due to first neighbor interractions.

Ethyl Bromide. Equilibrium isotherms for ethyl bromide in polyvinyl acetate at 30°, 40°, and 50°C. (Table 1) are presented in Figure 2 in the form V_1 vs. P/P_o. Up to about 0.2 relative pressure Henry's Law is obeyed. Also there appears to be no measurable heat of solution since all three isotherms coincide. The calculated Flory-Huggins parameters (Table 1) average .55 and show no decided trend with temperature either. Ethyl bromide, then, forms a moderately ideal solution with the polymer.

In view of this behavior, the cohesive energy density CED of the polymer may be calculated. This is defined[14] as the molar cohesion energy CE divided by molar volume. For normal liquids

$$CE = \Delta H_v - RT \qquad (13)$$

where ΔH_v is the experimentally determined molar heat of vaporization, which of course is not determinable for high polymers. However, according to Scatchard and Hildebrand[14], CED's for two substances are equal when their heat of mixing is zero. For ethyl bromide CED equals 79 cal/ml. at 30°C. (ΔH_v is 6600 cal/mole as calculated from Handbook vapor pressure data and the liquid density is 1.44 g/ml).

This value for polyvinylacetate is supported by Long's finding[13] that benzene (CED = 75 cal/ml) mixes athermally with the polymer but that for acetone (CED = 90 cal/ml) $\Delta \bar{H}_{1n}$ is -600 cal/mole. Moreover other extensive results[35] have given an average value of 77.6 cal/ml. These values are

Table 1

Summary of Equilibrium Sorption Results for Ethyl bromide in Polyvinyl Acetate

P/P_o	W	V_1	χ_1
	At 30°C		
.0599	.0159	.0126	.57
.0721	.0220	.0175	.45
.136	.0390	.0305	.54
.171	.0480	.372	.57
.248	.0768	.0583	.51
.310	.102	.0759	.49
.206	.0608	.0468	.58
.136	.0363	.0284	.63
			Average = .54
	At 40°C.		
.0949	.0255	.0203	.59
.127	.0363	.0285	.56
.157	.0447	.0349	.57
.0649	.0167	.0134	.61
.213	.0628	.0484	.55
			Average = .58
	At 50°C.		
.0549	.0154	.0124	.50
.0761	.0218	.0174	.50

Table 1 (cont)

P/P_o	W	V_1	χ_1
		At 50°C. (cont)	
.0980	.0278	.0222	.52
.121	.0353	.0279	.53
			Average = .51

Average χ_1 for all temperatures = .55

At 30° $v_1 = 0.695$ W ml., $v_2 = 0.862$ ml.

At 40° $v_1 = 0.705$ W ml., $v_2 = 0.871$ ml.

At 50° $v_1 = 0.715$ W ml., $v_2 = 0.878$ ml.

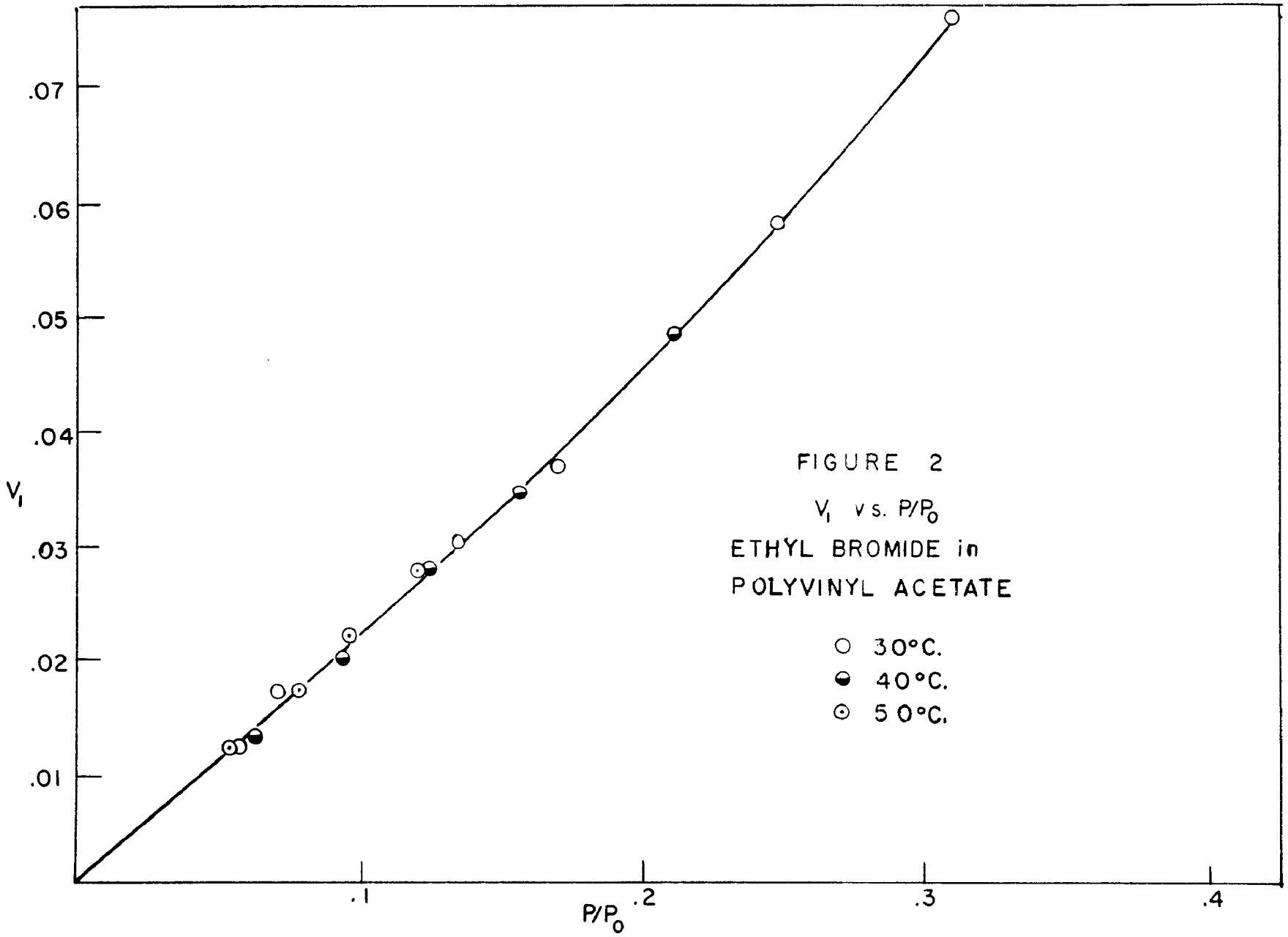
.07
.06
.05
.04
.03
.02
.01
V_1
.1
.2
.3
.4
P/P_0
FIGURE 2
V_1 vs. P/P_0
ETHYL BROMIDE in
POLYVINYL ACETATE
30°C.
40°C.
50°C.

contradicted by Meares' value of 86 cal/ml, calculated from calorimetric heats of dilution of polymer solutions.[15] However in these experiments polymer concentrations were never greater than 60%.

Acetonitrile. Extensive equilibrium data were taken for acetonitrile at 30° and 40°C. apart from the runs in which kinetics were studied. In part, this was required by the low accuracy of such data taken in the combination runs. Equilibrium determinations of comparable accuracy are more difficult in acetonitrile than in ethyl bromide because of the much lower saturation pressures of the former (e.g., 110 mm. vs 560 mm.).

Results (Table 2) are plotted in Figures 3 and 4 and immediately it is seen that the system is far from an ideal one. On the basis of the acetonitrile CED of 136 cal/ml. (ΔH_v = 7800, d = 0.772) non-ideality is expected. However close inspection reveals several dichotomies. First the average calculated values of χ_1 at 30° and 40°C (Table 2) are the same; that is, in spite of the large difference in cohesive energy densities, no heat of mixing appears. Two regions in the isotherms appear to be discernible, particularly in the one at 40°: an initial, small bump followed by a straight line.

The bump, if it is real, is reminiscent of a quasi-chemisorption. No explanation for this is available although it is tempting to speculate on such things as interraction between residual hydroxyl groups in the polymer and the highly polar nitrile group.

Table 2

Summary of Equilibrium Sorption Results for Acetonitrile in Polyvinyl Acetate

P/P_o	W	V_1	χ_1
	At 30°C.		
.260	.0473	.0663	.49
.362	.0737	.0997	.48
.428	.0937	.124	.47
.0246	.0046	.0069	.09*
.0430	.0091	.0135	.19*
.0837	.0146	.0215	.39
.117	.0218	.0317	.35
.172	.0300	.0432	.46
.233	.0418	.0590	.49
.272	.0519	.0722	.45
.315	.0619	.0852	.47
.374	.0773	.104	.47
.0298	.0045	.0067	.51
.0526	.0073	.0109	.59
.0881	.0127	.0188	.57
.128	.0210	.0306	.50
.183	.0328	.0470	.45
.221	.0400	.0566	.47

Average = .48

Table 2 (cont)

P/P_o	W	V_1	X_1
		At 40 °C.	
.0369	.0073	.0109	.23
.0975	.0155	.0229	.50
.154	.0264	.0383	.47
.230	.0419	.0595	.46
.311	.0592	.0821	.49
.286	.0555	.0773	.45
.259	.0483	.0679	.47
.211	.0392	.0559	.44
.179	.0318	.0458	.45
.130	.0218	.0319	.46
.0599	.0118	.0175	.26
.0180	.0036	.0054	.22
.0134	.0018	.0027	.61
.0360	.0064	.0096	.34
.0585	.0091	.0136	.56
.0983	.0146	.0216	.55
.0745	.0136	.0201	.33
.178	.0346	.0496	.37
.253	.0500	.0702	.42
.326	.0673	.0924	.42
.394	.0810	.1090	.51

Table 2 (cont)

P/P_o	W	V_1	χ_1
		At 40° C. (cont)	
.0724	.0091	.0136	.70
.160	.0264	.0384	.71
.273	.0510	.0716	.47
.329	.0665	.0913	.47
.444	.0974	.128	.49
.304	.0565	.0786	.51
.401	.0828	.111	.50
.0102	.0018	.0028	.32
.0363	.0055	.0082	.51
.0479	.0073	.0109	.50
.0957	.0146	.0216	.53
.0733	.0100	.0149	.63
.0736	.0091	.0136	.72
.0809	.0127	.0188	.49
.0241	.0046	.0069	.25
.0578	.0082	.0123	.58

Average = .46

Average χ_1 for both temperatures = .46

* Excluded from averages

At 30° C. v_1 = 1.295 W ml., v_2 = 0.862 ml/g

At 40° C. v_1 = 1.315 W ml., v_2 = 0.871 ml/g

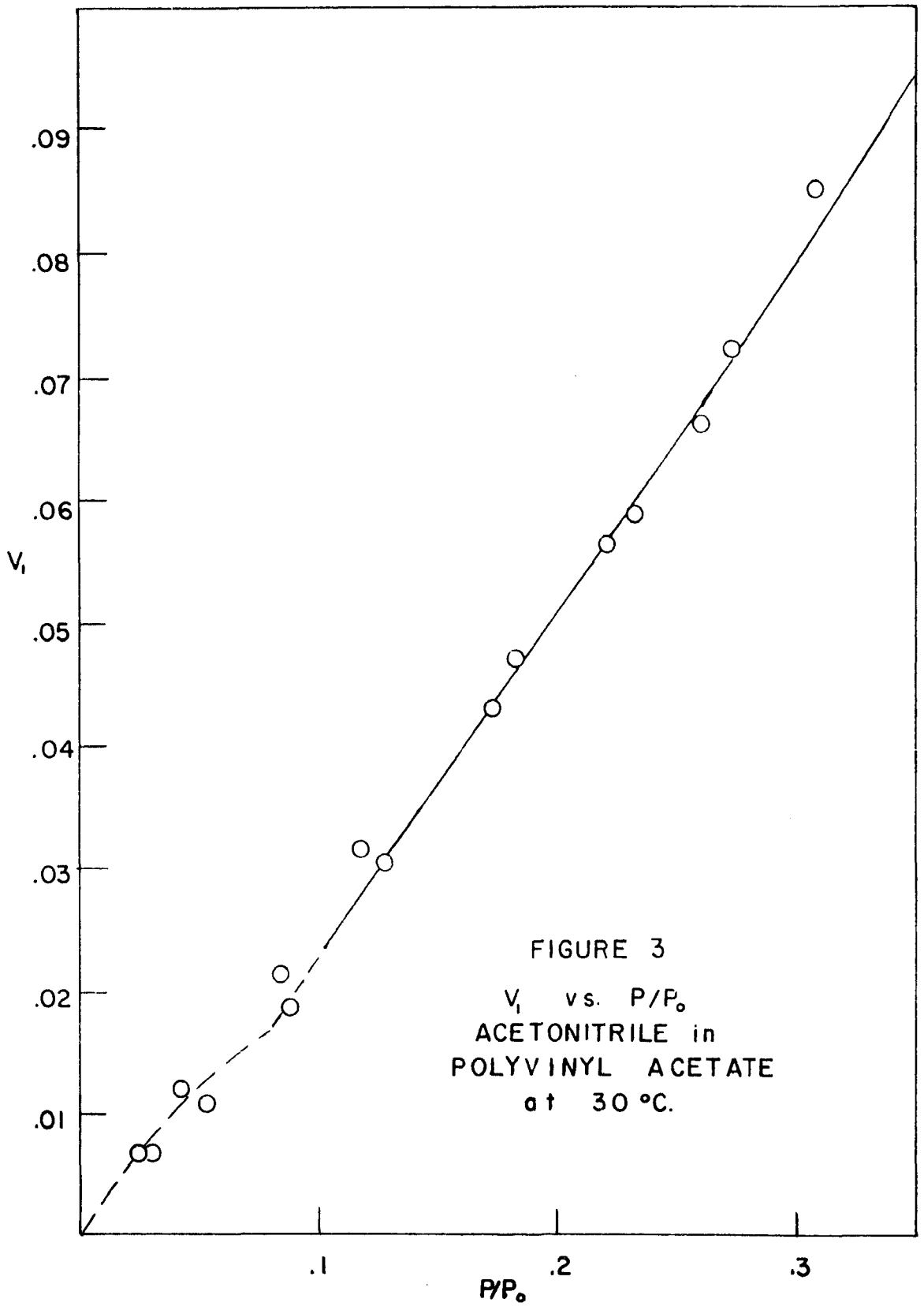

FIGURE 3

V_1 vs. P/P_o
ACETONITRILE in
POLYVINYL ACETATE
at 30 °C.

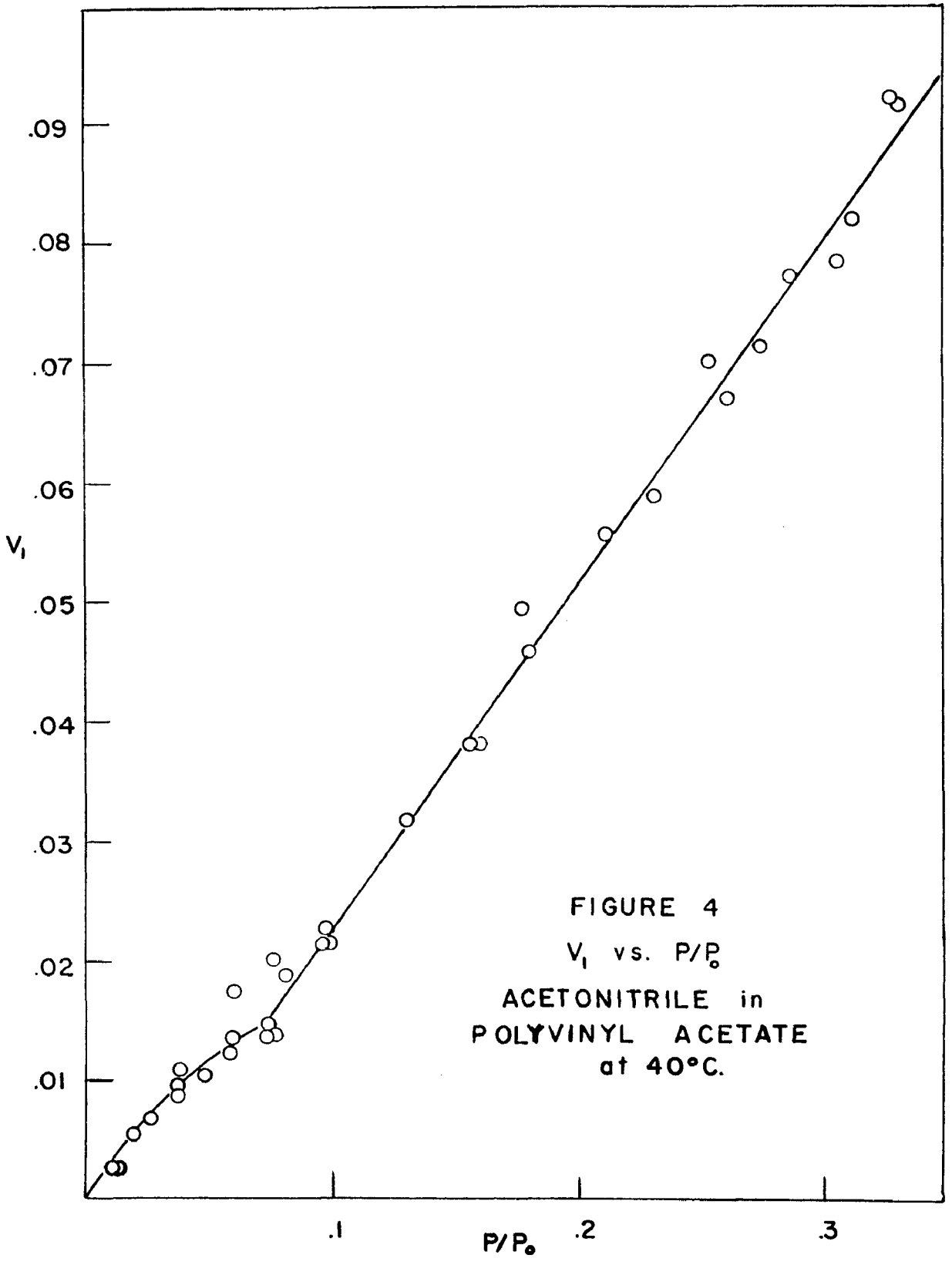

FIGURE 4

V_1 vs. P/P_o

ACETONITRILE in

POLYVINYL ACETATE

at 40°C.

The ensuing straight line portion with zero heat of solution is perhaps explanatory on the basis of the evidence[16] that acetonitrile exists as dipole pairs in the liquid, the energy of dissociation for which, has been estimated as 8 kcal/mole. (It does not dimerize in the gas phase as evidenced by a deviation from ideality of less than 1% at saturation pressure and 30°C, calculated from its critical constants.) Thus dipole pair re-formation in the polymer would be likely in which case the net change in interaction energy for each molecule in the transfer from liquid to polymer would be much less positive than expected otherwise. Stated another way, the vaporization of acetonitrile to gas-phase dipole pairs would involve much less than the experimental heat of vaporization and the corresponding liquid CED would be lower.

An interesting parallel to this situation is provided by propanol data[13] which yield a positive $\Delta \bar{H}_{ln}$ for solutions in polyvinyl acetate whereas the CED calculated from Handbook data in the above manner is 147 cal/ml. Alcohols are known[17] to be highly associated in solutions of carbon tetrachloride (CED = 75 cal/ml.) and methyl alcohol has even been shown to associate appreciable in the gas phase.[18]

Kinetic Results

Ideal Behavior. In Figure 5 are presented hypothetical ideal sorption and desorption curves for a vapor in an amorphous polymer above its glass temperature where

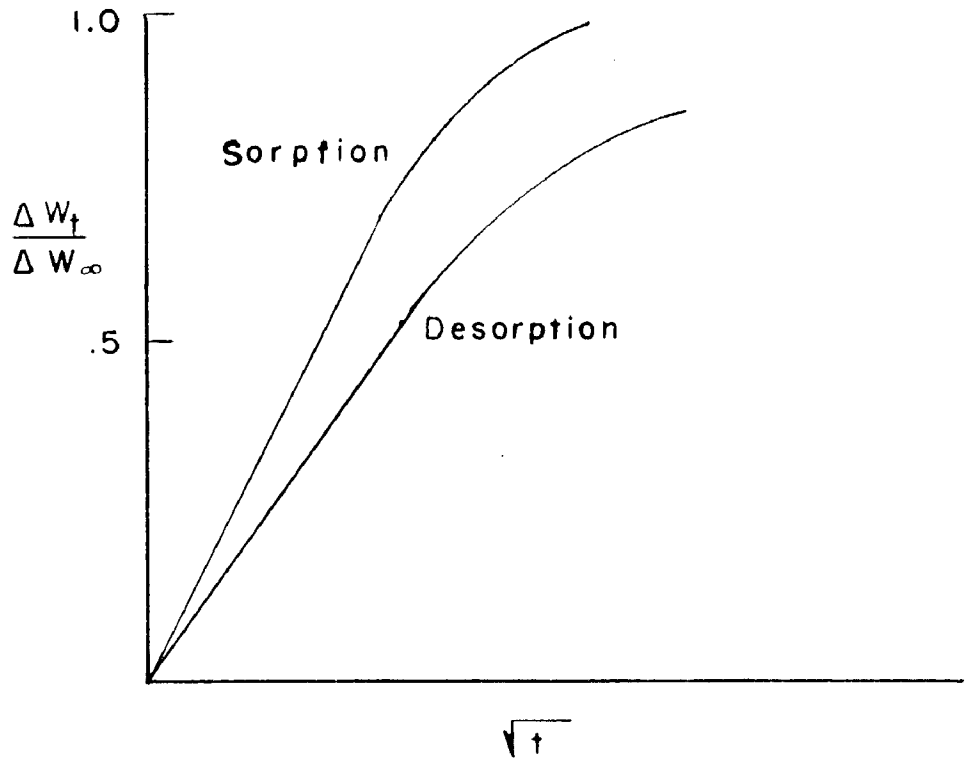

FIGURE 5

HYPOTHETICAL IDEAL SORPTION BEHAVIOR

the diffusion coefficient is an increasing function of concentration. It will be noted that the plot of fractional weight change against the square root of time is initially linear, the line passing through the origin in each case. In addition there is no inflection point anywhere in either curve in accordance with the requirements for Fickian behavior.[4] Finally, the desorption curve lies below the sorption curve at all times as is experimentally observed in general for organic vapors diffusing into polymers above their glass transition temperatures.[10] That this should be true is predictable from the mathematics of Fickian sorption when the diffusion coefficient is an increasing function of concentration.[8] This can be seen qualitatively for the comparison of the final approaches to equilibrium in the two cases. Here the concentrations of vapor at the film center have changed appreciably from their initial values, in one instance rising, in the other dropping. Thus when diffusion rates are compared at concentration gradients of equal magnitude (the only rate-controlling variable when $D = f(C)$) it is seen that the desorption rate is the lower of the two because diffusion here is occuring over an average concentration which is lower than that for the last stages of sorption.

Typical Results. In Figure 6 are plotted typical sorption-desorption data for ethyl bromide at 50°C. which illustrate one of the main experimental limitations, the inability to admit or evacuate the vapor in the column rapidly enough in terms of the sorption half-time. The sorption

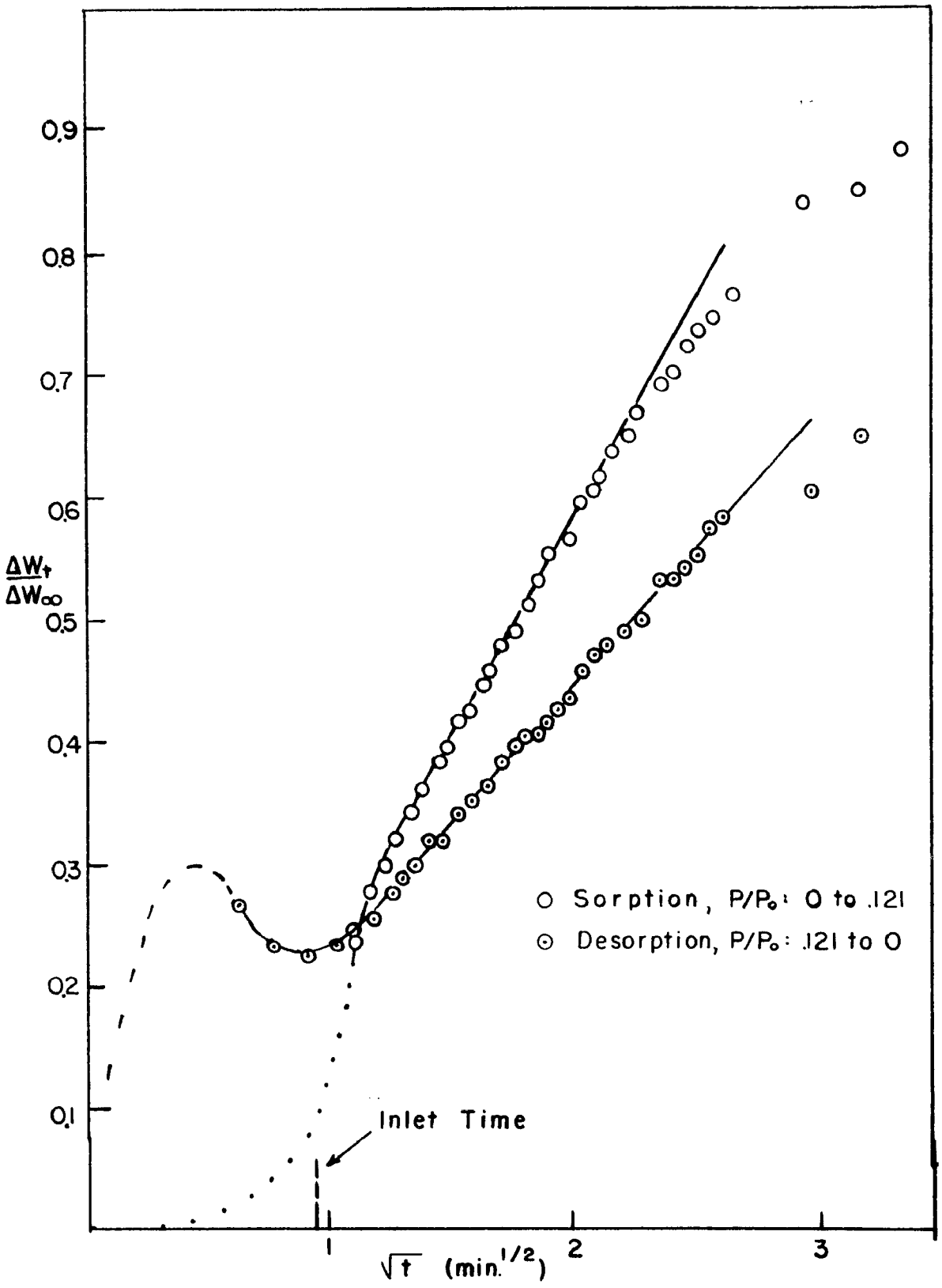

FIGURE 6
TYPICAL KINETIC RESULTS
RUN *15: ETHYL BROMIDE AT 50 °C.

curve is initially sigmoidal indicating a slow sorption rate at the beginning while the pressure is low, changing to a very fast rate as the pressure reaches its final value, and finally subsiding to what may be termed the normal rate. The slow initial rate is easily understandable in terms of the low ambient pressure. The change to the very fast subsequent rate with a final subsiding may be understood as the sorption process "catching up with itself". Figure 7 shows the concentration gradients of sorbed vapor in a film for a number of cases where the diffusion coefficients are concentration dependent to differing extents.[8] It will be noted that as the concentration dependence increases, a "front" of advancing vapor tends to form behind which the concentration gradient tends to vanish. That is, diffusion of vapor into polymer somewhat plasticized by vapor already present is quite rapid, whereas advancement of the "front" into dry polymer is slower and thus under steady-state conditions tends to be over-all rate determining. Therefore the initial sorption of a small amount of vapor in the surface layers of the film, allows a rapid second stage process terminated by the arrival at the "front", after which sorption proceeds in a normal fashion.

Desorption studies, of course, are potentially susceptible to the same difficulty but generally seemed to exhibit one of another cause instead. The desorption curve in Figure 6 appears to show an initial extremely rapid rise, a leveling off, a descent and finally a settling down to the

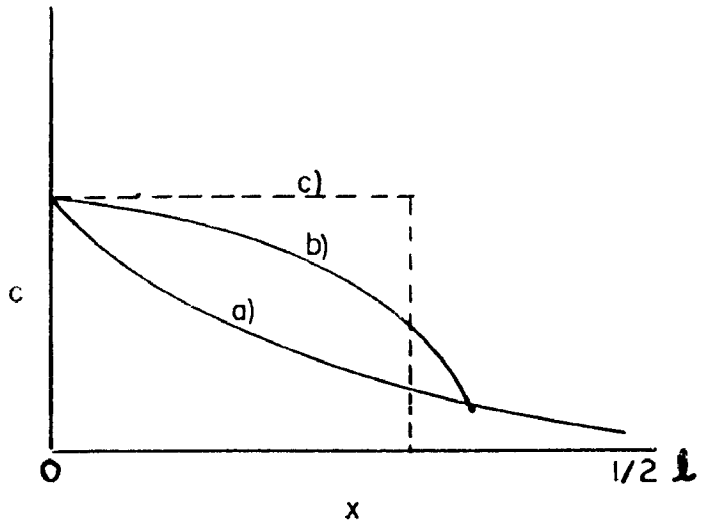

FIGURE 7

CONCENTRATION GRADIENTS FOR DIFFUSION COEFFICIENTS OF DIFFERENT CONCENTRATION DEPENDENCES

a) $\partial D/\partial c = 0$
b) $\partial D/\partial c = f(C)$
c) $\partial D/\partial c = \infty$

normal behavior. This roller coaster pattern originated in the movement of the spring in the vapor breeze set up by evacuation. Since the outlet was at the top of the column, evacuation caused an upward draft which lifted the spring and sample slightly. This lift abated as the pressure dropped and the spring returned to its proper extension.

With both sorption and desorption the initial abnormal data were ignored in the calculation of slopes. Generally, data up to 60 or 70 percent of the process were usable for calculations, after which curvature set in, its appearance coming sooner for desorption than for sorption.

Both of the above errors can be minimized by use of thicker films since the half time for both processes is inversely proportional to the film thickness. That such was not done for much of the work reported here was due to the fact that only late in the project was film production routine enough to insure a supply of film samples of requisite thicknesses. Nevertheless the experimental results obtained did not seem seriously impaired by these errors since, as will shortly be seen, they were found to be generally in harmony with other published work.

The final large inaccuracy lay in the sensitivity and accuracy of weight of sorbed vapor determinations. Owing to geometric limitations of the system and the thinness of the available film samples, these were often so light that ability to determine small percentage changes accurately was impaired. Also increasing skill in adjustment and use of the cathetometer resulted only near the end of the work

in attaining the sensitivity and reproducibility in readings attributed to the instrument.

Finally, some doubt appears to exist concerning the intrinsic ability to determine diffusion coefficients for organic vapors in polymers in the regions just above their glass temperatures by the sorption method.[19] Since the glass temperature is really a temperature range, "glassy" effects actually might influence rate processes for several degrees above the nominal glass temperature (e.g., as high as 40° for polyvinyl acetate according to one estimate,[20] 50° according to another[21]). Thus the instantaneous attainment of thermodynamic equilibrium of the polymer-vapor solution for each change in vapor concentration might not occur, and sorption would then be non-Fickian to some degree. However a comparison of results obtained near T_g with those at much higher temperatures (see page 79) shows no indication that the former are greatly suspect.

Dependence of Diffusivities on Concentration. In Figure 8 are plotted the logarithms of the integral diffusion coefficients for ethyl bromide against equilibrium weight sorbed per weight of polymer (Table 3) (cf. eqn. 7). The data for each of the three temperatures fit a straight line relationship with $\bar{D}$ increasing with concentration as expected. Line slopes (α_w) and intercepts have been calculated by the least squares method and are listed in Table 3. Figure 9 contains a similar plot for the less numerous acetonitrile data. The line slope and intercept are also contained in Table 4.

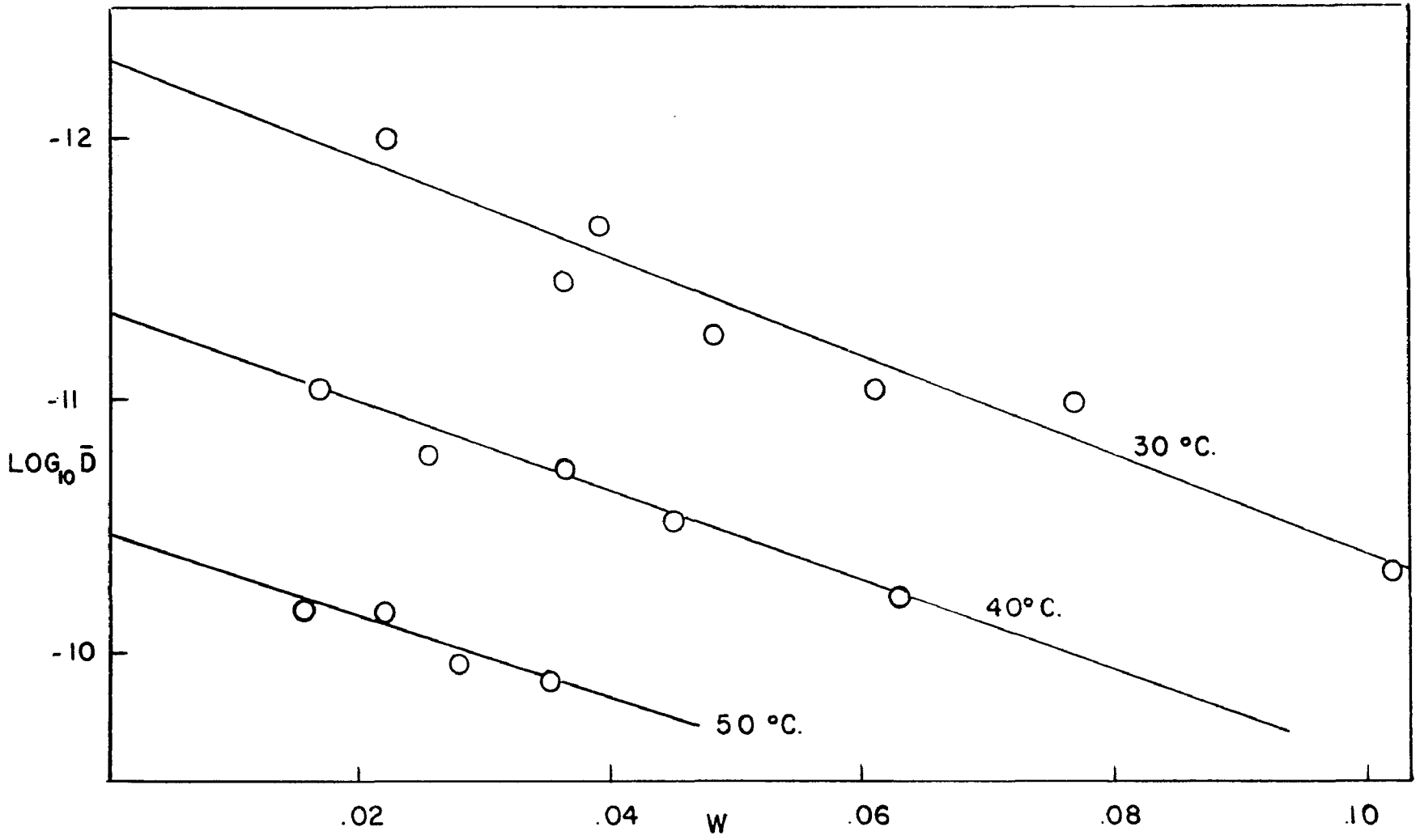

FIGURE 8

LOG_{10} $\bar{D}$ vs. W (g./g.)
ETHYL BROMIDE IN POLYVINYL ACETATE

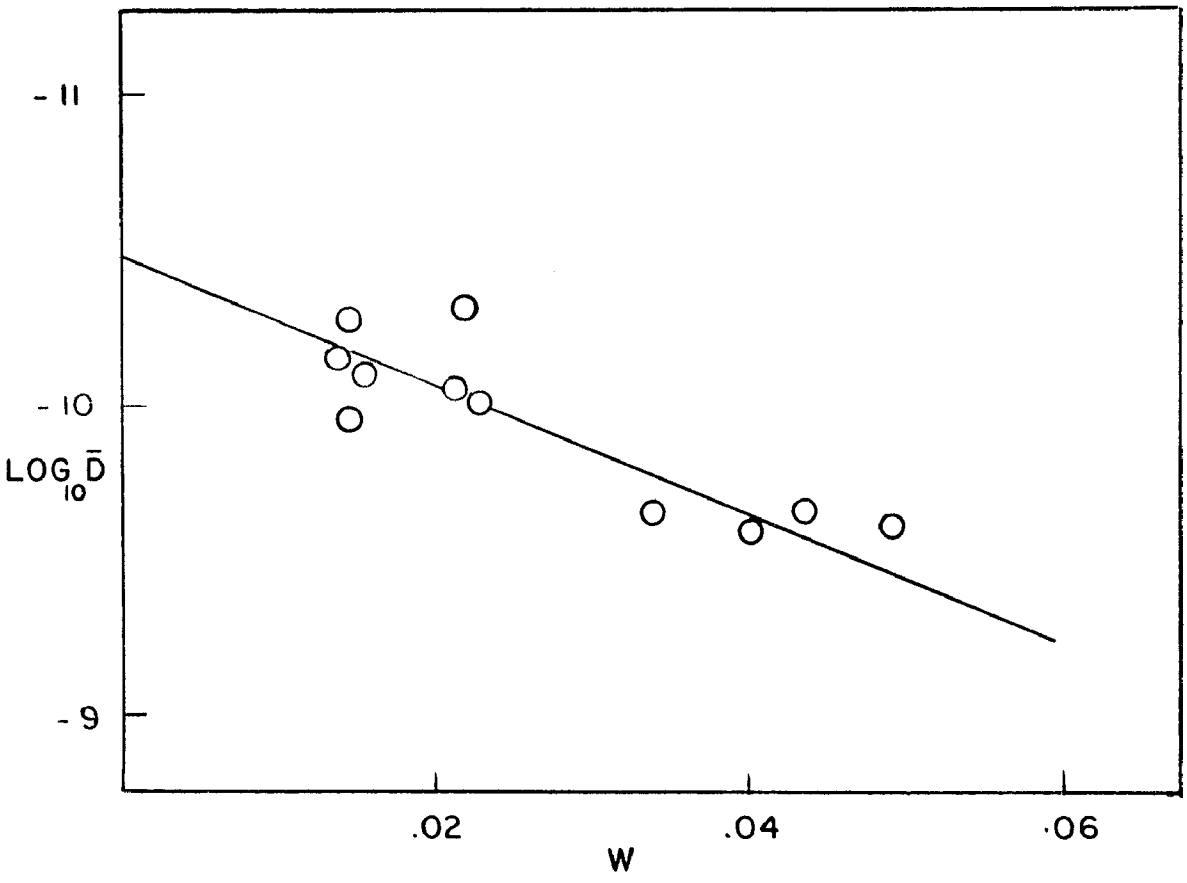

FIGURE 9

$LOG_{10}\ \bar{D}$ vs. W (g./g.)
ACETONITRILE IN POLYVINYL ACETATE
AT 30 °C.

Table 3

Summary of Diffusion Results for Ethyl bromide in Polyvinyl Acetate

P/P_o	W	V_1	$\bar{D} \times 10^{12}$ cm^2/sec
		At 30°C.	
.0599	.0159	.0110	1.01
.0721	.0220	.0153	1.01
.130	.0390	.0273	1.10
.171	.0480	.0333	5.56
.248	.0768	.0533	1.07
.310	.102	.0708	4.58
.206	.0608	.0422	8.99
.136	.0363	.0252	3.83
		$\log_{10} D_o = -12.30$, $\alpha_w = 44$, $\alpha_v = 63$	
		At 40°C.	
.0949	.0255	.0180	16.3
.127	.0363	.0256	18.7
.157	.0447	.0315	29.2
.0649	.0167	.0118	9.39
.213	.0628	.0442	58.2
		$\log_{10} D_o = -11.29$, $\alpha_w = 38$, $\alpha_v = 55$	
		At 50°C.	
.0549	.0154	.0138	65.4
.0761	.0218	.0195	66.4

Table 3 (cont)

P/P_o	W	V_1	$\bar{D} \times 10^{12}$ cm^2/sec
	At 50°C. (cont)		
.0980	.0278	.0247	100.7
.121	.0353	.0284	125.8

$\log_{10} = -10.46$, $\alpha_W = 36$, $\alpha_V = 46$

Table 4

Summary of Diffusion Results for Acetonitrile in Polyvinyl Acetate at 30°C

P/P_o	W	V_1	$\bar{D} \times 10^{-11}$ cm^2/sec
.0864	.0137	.0201	6.9
.190	.0337	.0481	22
.267	.0491	.0687	37
.119	.0209	.0305	8.8
.220	.0400	.0566	25
.124	.0217	.0330	9.8
.230	.0433	.0611	21
.153	.0264	.0382	7.8
.123	.0218	.0319	4.8
.0868	.0146	.0214	11
.0947	.0146	.0214	5.2

$\log_{10} = -10.48$, $\alpha_W = 48$, $\alpha_V = 34$

Long has suggested a linear relationship between log D_0 and molar volume of the organic liquid (discussed further on) and Figure 10 is such a graph of his data for 30°C and the ethyl bromide and acetonitrile points from this work. Agreement seems quite good.

Long has also suggested that a relationship exists between the line slope α_v for the plot of $\log_{10} \bar{D}$ vs concentration in volume fraction units, and the Flory Huggins parameter. (For the calculation of α_v it is necessary to assume volume additivity[10], in which case $V_1 = (W/d_1)/(W_1/d_1 + 1/d_2)$). His plot of α_v against χ_1 at 40°C. is reproduced in Figure 11 and on it is superimposed the ethyl bromide point at 40° from this work. Agreement is again good.

The value of α_v for acetonitrile at 30° calculated from Figure 9 seems somewhat questionable. Calculations for acetone, benzene, and propanol, from Long's data, and ethyl bromide from data taken here, show that α_v does not change drastically with temperature. On this basis and the non-variance of α_v for acetonitrile with temperature, it might be expected that the location of a point for this vapor at 30° on Figure 11 would be near the 40° line. That it would not fall near the line may be due, in part at least, to the growth in seriousness of the experimental error connected with the problem of inlet and evacuation times resulting from the much faster diffusion rate of acetonitrile relative to ethyl bromide. It is likely, however, that part of the discrepancy is attributable to non-additivity of vo-

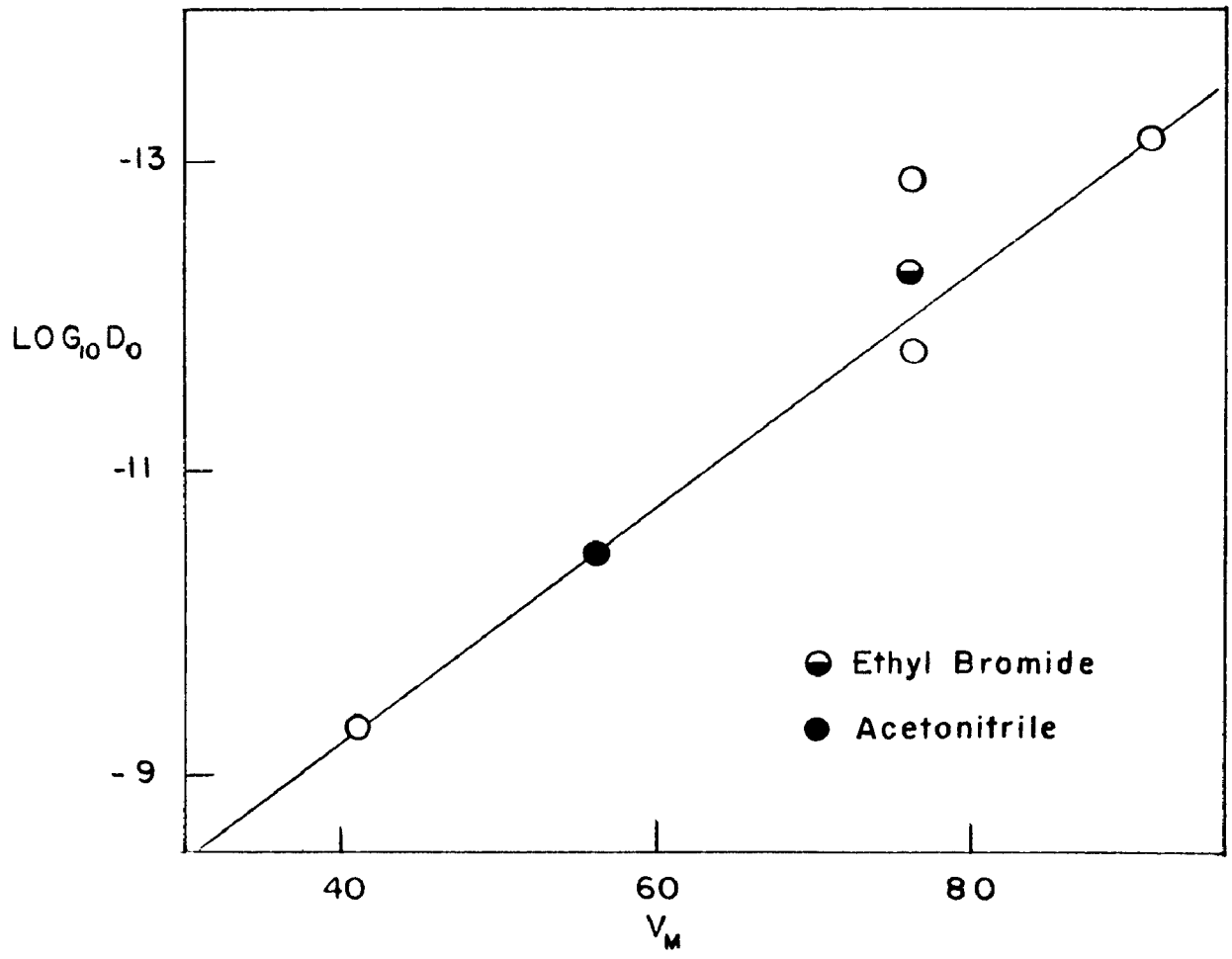

FIGURE 10

$LOG_{10}\ \bar{D}_0$ vs. V_M AT 30°C.

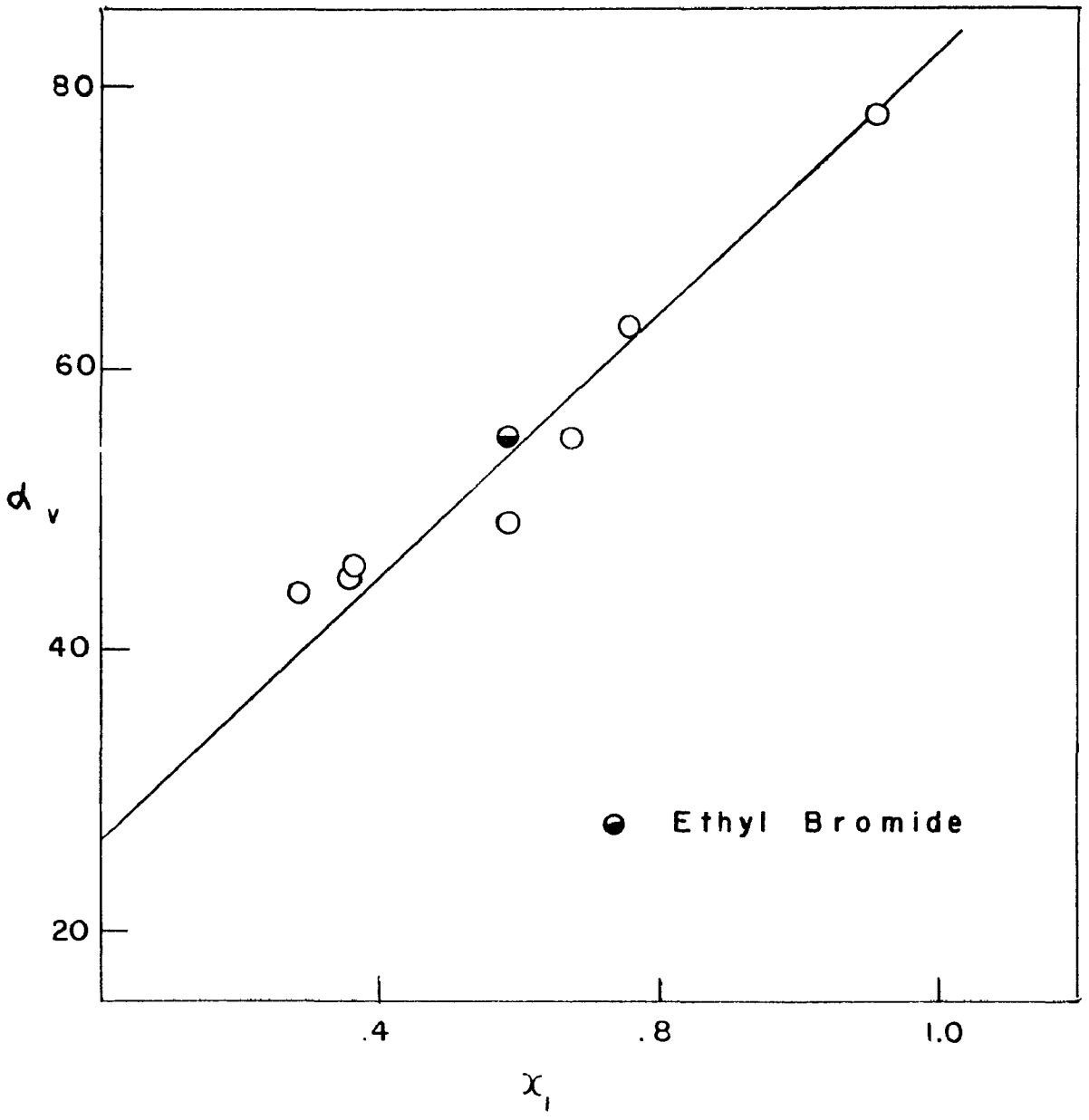

FIGURE II

α_v vs. x_1 AT 40°C.

lumes in this vapor-polymer system due to the widely different cohesive energy densities. In this connection it is interesting to note that an α_v of 18 for methanol at 40° may be calculated from Long's data, which value falls far below the line in Figure 11. The cohesive energy density for methanol (195 cal/ml.) is much higher than that for the polymer also.

Activation Parameters for Diffusion. In Figure 12 are plotted the logarithms of the true diffusion coefficients for ethyl bromide against the reciprocal of absolute temperature for volume fractions of the vapor equal to zero, .03, and .06. Those for zero concentration are simply the limiting values taken from Figure 8. The true diffusion coefficients for the .03 and .06 volume fractions were calculated from (8), using the values of α_v in Table 5. The activation energies for diffusion at the three concentrations were calculated from the equation[22]

$$\ln D / \quad (1/T)_{v_1} = -\Delta E^{\ddagger}/R \qquad (13)$$

and are listed in Table 5. The value of 41 kcal/mole for the dry polymer compares well with the extrapolation of other results obtained at higher temperatures as will be seen shortly.

In terms of the theory of absolute reaction rates[22] the diffusion coefficient is given by

$$D = e\lambda^2 \quad (kT/h)\, e^{\Delta S^*/R}\, e^{-\Delta E^*/RT} \qquad (14)$$

where e is the Naperian logarithm base, λ is the length of the unit diffusion step, and ΔS^* the activation entropy.

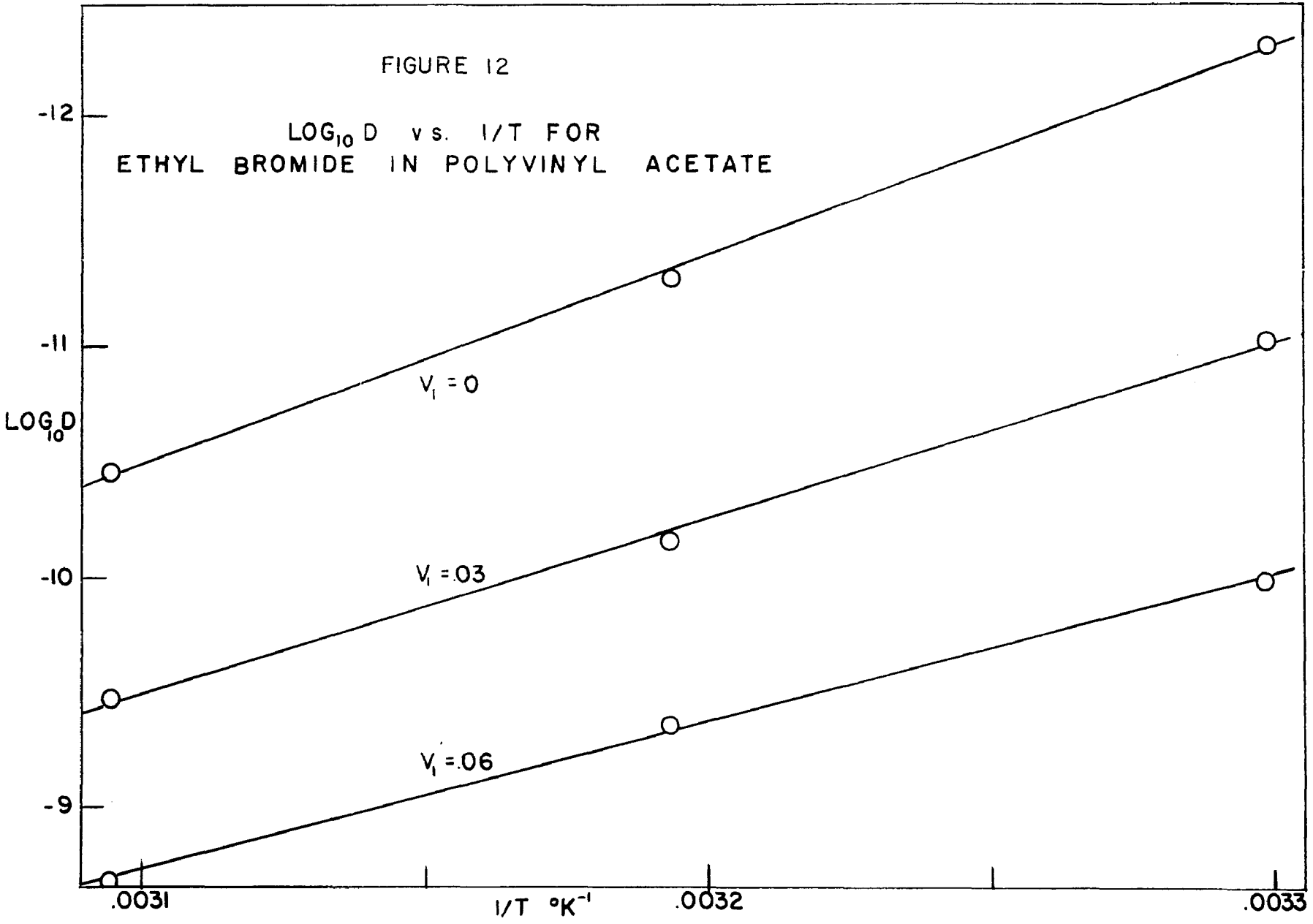
FIGURE 12
LOG10 D vs. 1/T FOR
ETHYL BROMIDE IN POLYVINYL ACETATE
-12
-11
-10
-9
LOG10D
V1 = 0
V1 = .03
V1 = .06
.0031
.0032
.0033
1/T °K-1

Table 5

Various Parameters Relevant to the Concentration and Temperature Dependences of the Diffusion of Three Vapors in Polyvinyl Acetate

	Acetone	Benzene	Ethyl Bromide
α_v (30°)	63	44	63
α_v (40°)	55	46	55
α_v (50°)	50	43	46
$\Delta E^{\ddagger}$ ($V_1 = 0$)	41.6	35.5	41
$\Delta E^{\ddagger}$ ($V_1 = .03$)	39	35.0	41
$\Delta E^{\ddagger}$ ($V_1 = .06$)	—	35.5	29
$\Delta S^{\ddagger}$ ($V_1 = 0$)	80.5	55.0	74
$\Delta S^{\ddagger}$ ($V_1 = .03$)	78	57.7	59
$\Delta S^{\ddagger}$ ($V_1 = .06$)	—	60.8	47
V_f (cc/cc)	.0030	.0024	.0076

The other symbols have their usual significance. Assuming a path length allows the calculation of $\Delta S^{\ddagger}$. A value of 30 Å has been chosen in line with discussion in the next section; although this is a risky assumption, a large variation in λ has a small effect on $\Delta S^{\ddagger}$ because of the form of (14). Values for $\Delta S^{\ddagger}$ at 40°C and the various concentrations have been calculated in this way and are listed in Table 5.

The calculation of $\Delta E^{\ddagger}$ and $\Delta S^{\ddagger}$ at the different concentrations has also been done, in the ways described above, for benzene and acetone from graphs presented in Long's papers;[4,10] and these are listed in Table 5. It is to be noted that in contrast to the behavior of these two vapors, ethyl bromide vapor appears to cause a marked decrease in both activation energy and activation entropy. Long[43] has concluded that when vapor introduction into the polymer changes the diffusion activation parameters it does so primarily by changing the free volume fraction of the system. An increase in this quantity would be expected to lower the diffusion zone size[19].

Following this suggestion an attempt has been made to determine the effect of vapor introduction on the free volume fraction of the diffusion system for the vapors acetone, benzene, and ethyl bromide. Free volumes for these in their liquid states have been calculated by the following equation[44]

$$\Delta S_v = R \ln V_v/v_f \qquad (15)$$

Here S_v is the entropy of vaporization, V_v is the volume

of one mole of vapor under its vapor pressure, and v_f is the free volume of one mole of liquid. The free volume fraction V_f of the liquid is then given by

$$V_f = \frac{v_f}{(v_f + V_M)} \cong v_f/V_M \qquad (16)$$

where V_M is the molar volume of the liquid. In Table 5 are listed the free volume fractions in these organic liquids at 40°C. If volume additivity of polymer and vapor is assumed again, it is seen that ethyl bromide introduction would appear to increase the free volume fraction in the polymer-vapor system to a much larger extent than would introduction of the other two. Long's theory appears to be buttressed by these data, therefore.

THEORY OF LIMITING DIFFUSION IN LINEAR, AMORPHOUS HIGH POLYMERS

IV. THEORY OF LIMITING DIFFUSION IN LINEAR AMORPHOUS HIGH POLYMERS

Introduction

What follows is an attempt to extend the development of a unified picture of limiting diffusivities in linear amorphous polymers above their glass transitions, based primarily on contributions by F. A. Long[10] and P. Meares,[6] and utilizing their data plus those of G. Ya. Ryskin[25] (Tables 6 and 7). These contributions were made in the framework of the Eyring hole theory of diffusion[22] which holds as its main article of faith that diffusion processes in the liquid or solid state are activated ones in which the unit step is the formation of a hole in the medium adjacent to the diffusing particle, which then "jumps" into the hole.

Diffusion in ordinary liquids is generally accompanied by activation energies of roughly 5-10 kcal,[22] whereas diffusion in polymeric substances often involves activation energies in the neighborhood of 40-50 kcal. At one time it was thought that such high energies were due to bond breaking, but at present it is felt that the unit diffusion step requires the activation of a considerable volume or zone in the polymer, the actual activation energy density still remaining fairly small.[19] Both polymeric diffusion and viscous flow are considered at present to be processes wherein movement occurs by motion of chain segments rather than whole macromolecules.[6,22]

Table 6

Activation Data for Diffusion of Gases

in Polyvinyl Acetate at 300 °K

Gas	$\Delta E^{\ddagger}$ (kcal/mole)	$\Delta S^{\ddagger}$ (e.u./mole)
He	5.4	−6.2
H_2	7.5	−1.7
Ne	8.5	0.6
O_2	14.3	13.7
A	16.3	17.9
Kr	19.4	24.0
CH_4	19.3	24.6

Table 7

Activation Data for Diffusion of Vapors in

Six Linear Amorphous Polymers

above Their Glass Transitions

	Vapor	$\Delta E^{\ddagger}$ (kcal/mole)	$\Delta S^{\ddagger}$ (e.u./mole)
1.	In polyvinyl acetate. (T_g = 303 °K)		
	H_2O	13.8	20
	CH_3OH	20.5	34
	C_2H_5OH	28.5	53
	n−C_3H_7OH	31.0	55
	n−C_4H_9OH	35.9	68
	2−C_4H_9OH	36.0	67
	3−C_4H_9OH	36.2	67

Table 7 (cont.)

Vapor	$\Delta E^{\ddagger}$ (kcal/mole)	$\Delta S^{\ddagger}$ (e.u./mole)
CH_3COCH_3	32.0	60
C_6H_6	38.0	75
C_5H_5N	35.0	67
cyclo C_6H_{12}	38.6	75
CH_2Cl_2	31.7	61
$CHCl_3$	36.4	72
CCl_4	38.7	77
C_2H_5Cl	31.9	60
C_2H_5Br	34.0	63
C_2H_5I	36.4	71
2. In polystyrene. (T_g = 361 °K)		
CH_3OH	17.5	25
C_2H_5OH	21.0	28
CH_2Cl_2	24.0	35
C_2H_5Br	26.0	39
3. In polyethyl methacrylate (T_g = 313 °K)		
H_2O	10.1	9.2
CH_3OH	14.7	17
C_2H_5OH	20.2	27
C_6H_6	27.6	40
C_5H_5N	27.1	39

Table 7 (cont.)

Vapor	$\Delta E^{\ddagger}$ (kcal/mole)	$\Delta S^{\ddagger}$ (e.u./mole)
4. In polymethyl acrylate (T_g = 280 °K)		
H_2O	12.4	17
CH_3OH	17.0	27
C_2H_5OH	23.9	44
C_6H_6	25.8	45
5. In polymethyl methacrylate (T_g = 363 °K)		
H_2O	14.8	19
CH_3OH	21.6	29
C_2H_5OH	28.5	41
6. In polybutyl methacrylate (T_g = 283 °K)		
CH_3OH	12.0	17
C_2H_5OH	14.0	20

Effect of Molecular Size on Diffusion

If diffusion involves hole formation it would be natural to expect some sort of relationship between the size of the diffusing entity and the hole size as it influenced the activation energy. For diffusion in normal liquids simple relationships of this kind do not exist although the tendencies are noticeable. The reasons for this are discussed elsewhere.[22] Simple relationships do not exist in general for rubbers,[24] or partially crystalline polymers as will be discussed below. However Long[19] showed that for diffusion of organic vapors in polyvinyl acetate above T_g, the logarithm of the limiting diffusion coefficient decreased in proportion to the increase in the molar volume of the organic liquid, the latter being a measure of the size of the individual organic molecule. Shortly thereafter Meares,[6] in an extensive study of diffusion and permeability of permanent monatomic and diatomic gases in polyvinyl acetate showed the activation energies to be directly proportional to collision cross-sectional areas but that such a plot against the collision volumes was curvilinear. From this it was concluded that the size of the diffusant controlled the hole cross-sectional area but that the hole length was constant. Since the hole seemed roughly to be a cylinder of constant length but varying cross-sectional area, and since the volume of the hole might be proportional to the ratio of the activation energy and the cohesive energy density, the following expression for the hole length was proposed

$$L = E / [(CED)\ N\ (CSA_o)] \qquad (17)$$

CED, N, and CSA_o stand for cohesive energy density, Avogadro's number, and collision cross-sectional area respectively. Using a cohesive energy density for polyvinyl acetate of 90 cal/ml., hole lengths of 24 to 28 A were calculated, the average being 27 A with no discernible trend in length between hydrogen and methane.

In light of these findings it seemed natural to look for a correlation between permanent gas diffusion and that of the larger organic molecules. In Figure 13 are plotted diffusion activation energies for the seven permanent gases,[6] and seventeen vapors[25] against their liquid molar volumes as calculated from liquid densities given in the Handbook of Chemistry and Physics. Although the organic vapor data fit a smooth curve, it is not linear; the permanent gas points scatter quite badly.

In Figure 14 Meares' plot of activation energy vs collision cross-sectional area for the gases (Table 8) is reproduced. On it are superposed similar points for the organic vapors wherever values of collision areas are known (Table 8). It will be seen that, although there is appreciable scatter, the points do fall evenly about the extrapolated line. The scatter is undoubtedly due to the difficulties involved in determining collision diameter. This successful superposition indicates that limiting diffusion of all species, at least up to the size of benzene and ethyl bromide, involves a single mechanism, whether or not the details of it as de-

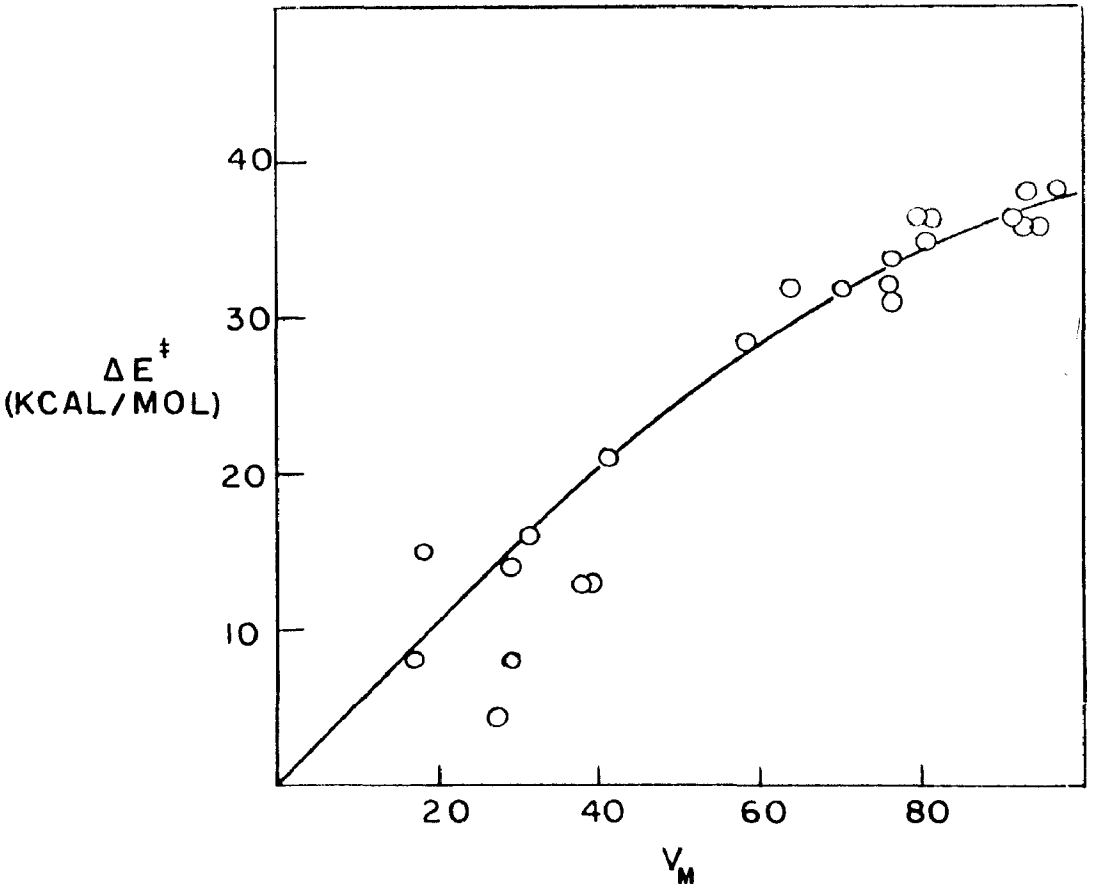

FIGURE 13

$\Delta E^{\ddagger}$ vs. V_M

DIFFUSION IN POLYVINYL ACETATE

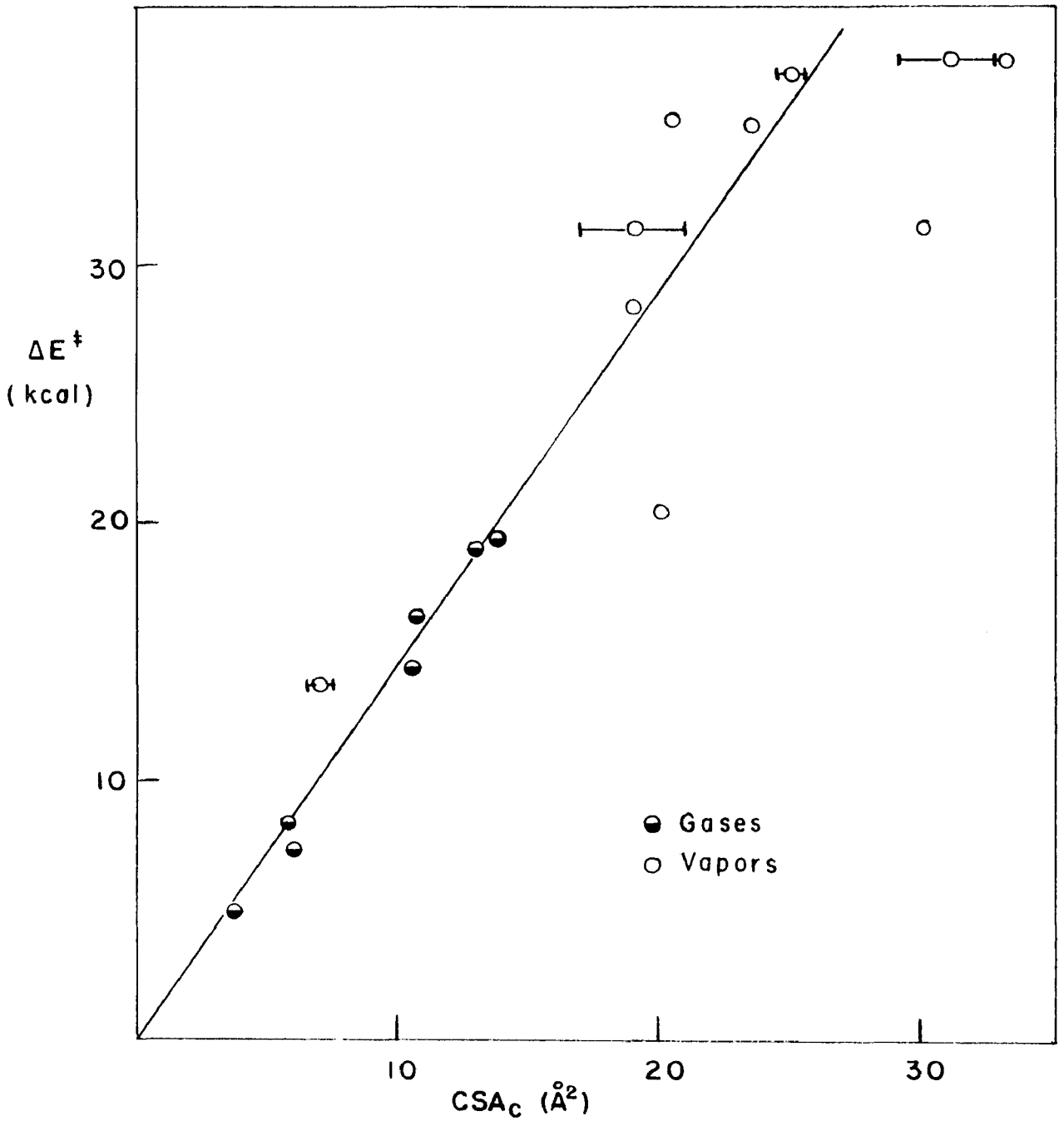

FIGURE 14

$\Delta E^{\ddagger}$ vs. CSA_c
DIFFUSION IN POLYVINYL ACETATE

Table 8

Molecular Size Data

Molecule	Diffusion CSAc (A^2)[†]	V_M (ml)	Parachor	CSAp (A^2)	"True" CSAc (A^2)
He	3.73[a]	27	19.2*	5.93	
H_2	5.00[a]	29	35.1*	8.90	
Ne	7.30[a]	17	24.2*	6.99	
O_2	10.3[a]	28	54.0*	11.9	
A	10.5[a]	29	53.9*	11.8	
Kr	13.6[a]	39	69.8*	14.1	
CH_4	13.1[a]	22	69	14.0	
CO_2	15.0[b]	—	—	—	
H_2O	6.5–7.5	18	46.7	10.6	9.5
CH_3OH	20[d]	42	85	16.0	14.0
C_2H_5OH	19–26[d,h]	58	124	20.6	19.5
n–C_3H_7OH	32[d]	76	163	24.9	
n–C_4H_9OH	23.5[d]	94	201	28.8	
2–C_4H_9OH	29–33[d]	92	201	28.8	
3–C_4H_9OH	—	92	201	28.8	
CH_3COCH_3	17[e]**	76	162*	24.6	
C_6H_6	24.5–25.5[g]**	91	206*	28.8	26.0
C_5H_5N	—	81	187	27.2	24.0
cyclo C_6H_{12}	33–40[ef]**	93	332	40.0	
CH_2Cl_2	—	64	143*	22.7	22.0

Table 8 (cont.)

Molecule	Diffusion CSAc (A^2)†	V_M (ml)	Parachor	CSAp (A^2)	"True" CSAc (A^2)
$CHCl_3$	20.5[e]**	80	183*	26.8	
CCl_4	29–33[f]	97	220*	30.2	
C_2H_5Cl	—	70	157	24.3	
C_2H_5Br	—	76	168*	25.3	25.0
C_2H_5I	—	81	181	26.4	

†CSA calculated in c through g by Kelvin's equation, p250, S. Chapman and T. G. Cowling, Mathematical Theory of Non – Uniform Gases, The University Press, Cambridge, England, 1939.

*observed; others calculated.

**σ^2_{air} assumed = $1/5\,\sigma^2_{O_2} + 4/5\,\sigma^2_{N_2}$

[a] Ref. 6, 41; [b] Ref. 23; [c] F. A. Schwertz and J. E. Brow, J. Chem. Phys. 19 640 (1951); [d] Int. Crit. Tables data for diffusion into CO_2 plus above value for CSA of CO_2; [e] N. A. Goryunova and E. V. Kuvshinskii. Zhur. Tekh. Fiz. 18 1421 (1948), Chem Abstr. 45 9957a (1951); [f] G.A. McD. Cummings and A. R. Ubbelohde, J Chem. Soc. 1953 3751; [g] C. R. Wilke and C. Y. Lee, Ind. and Eng. Chem. 47 1253 (1955).

σ's for O_2 and H_2 from Ref. 28.

veloped here are correct.

If the activation energies for the gases and vapors are plotted against the two thirds power of the molar volume (a measure of molecular cross-sectional area) a straight line is obtained; however, as with the plot against the first power of volume, the permanent gases are not well correlated by this procedure. That they are not is perhaps due to the fact that the densities taken correspond to states of widely differing internal pressure.

To overcome these discrepancies the use of the parachor has been suggested.[20] Parachors are calculated by means of the equation[26]

$$P = M \gamma^{1/4} / (d_l - d_v) \qquad (18)$$

where P is the parachor, M the molecular weight, γ the liquid surface tension, d_l the liquid density, and d_v the density of the vapor in equilibrium with the liquid. Parachors are measures of molecular volumes for temperatures at which the liquid surface tensions are equal. The molecular volume for non-metallic liquids at zero degrees Kelvin is given by[27]

$$v_o = 0.346\ P \qquad (19)$$

The parachor values used were literature values or ones calculated by the method of summations using atomic parachor values. From them cross-sectional areas were calculated for the molecules assuming spherical shape, by means of (19) and the assumptions that

$$v_o = 4 \pi r^{-3} \qquad (20)$$

$$CSA_p = \pi r^{-2} \qquad (21)$$

where CSA_p denotes the molecular cross-sectional area derived from the parachor and $\bar{r}$ is some sort of effective molecular radius.

Table 8 lists the parachors and the cross-sectional areas derived from them. Figure 15 is a plot of diffusion activation energy against parachor cross-sectional area for the gases and vapors in polyvinyl acetate. For comparison the line for activation energy against collision cross-sectional areas is included. The agreement is quite satisfactory, even more so than appears at first sight. Experimentally-determined molecular diameters have values dependent on the method of measurement;[28] values obtained from gaseous diffusion studies frequently differ from those from gas viscosity determinations under the same conditions for example. In addition diameters from gaseous diffusion studies vary with temperature due to the "sponginess" of the molecules, the higher temperature corresponding to the lower diameter; it is thus not surprising that collision diameters calculated from high temperature measurements would be smaller than those supposed to be effective at absolute zero. Finally as pointed out by Jeans, the average radius calculated from any kind of volume measurement will not, in principle even, be quite the same as that obtained from an experiment such as diffusion study which "sees" molecular silhouettes, and then only in a complicated fashion.

In Table 7 are listed activation energies for diffusion of a number of vapors in five other linear amorphous polymers above their glass transition temperatures.[25] These

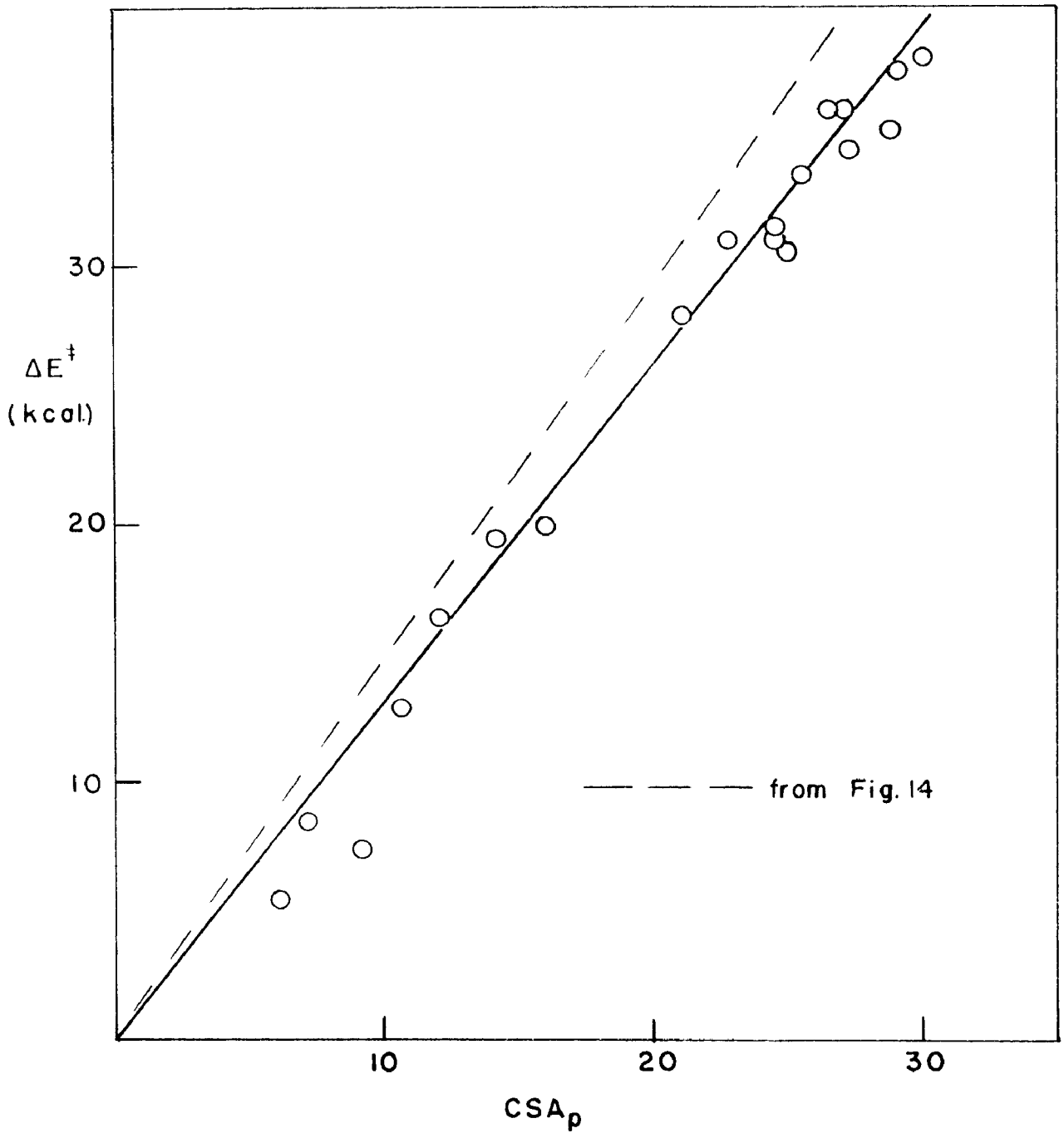

FIGURE 15
$\Delta E^{\ddagger}$ vs. CSA_p
DIFFUSION IN POLYVINYL ACETATE

results are plotted against parachor cross-sectional areas in Figures 16-18. Although the data are scarcer, it seems clear that in all cases the results can be correlated in the same way as for polyvinyl acetate.

Hole Lengths of the Unit Diffusion Processes

In order to use (17) to calculate hole lengths, polymer cohesive energy densities must be known. In line with the discussion concerning ethyl bromide isotherms, a value of 77.4 cal/ml will be used for polyvinyl acetate (cf. p. 19).

Experimental values of cohesive energy density for the other polymers do not seem to be available but they have been calculated using a modification of the group contribution method as discussed by Bunn.[29] This method utilizes the concept that molar cohesive energies are additive summations of group contributions. Using the group contribution terms derived for normal liquids,[29] cohesive energies per mole of chain units were calculated and are listed in Table 9. From these, the chain unit molecular weights, and the polymer densities, values for the polymer cohesive energy densities can be calculated, by means of

$$CED_{(calc.)} = CE\ (d/M) \qquad (22)$$

It will be noticed that the calculated values for polystyrene and polyvinyl acetate are appreciably lower than experimental values. However it is also known that molar cohesive energies themselves depend on densities, increasing as the latter increase.[29] Since the group contribution terms are

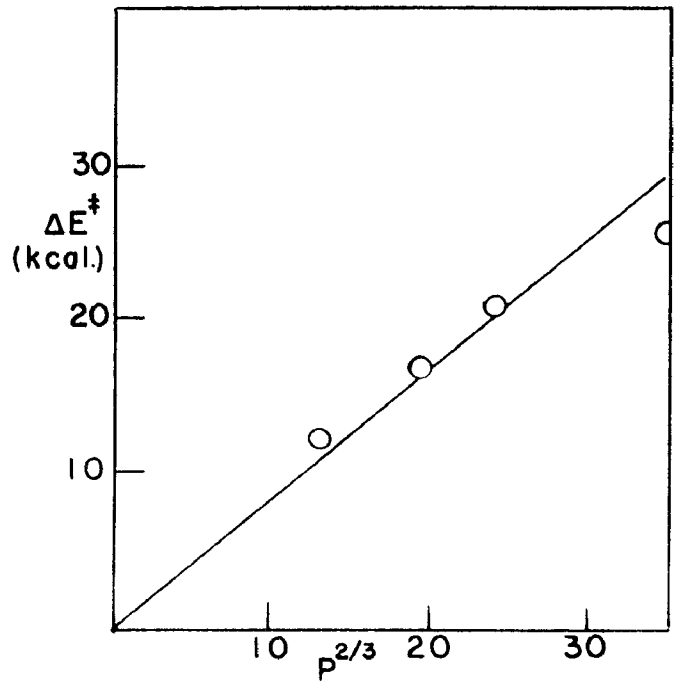

FIGURE 16
$\Delta E^{\ddagger}$ vs. $P^{2/3}$
POLYMETHYL ACRYLATE

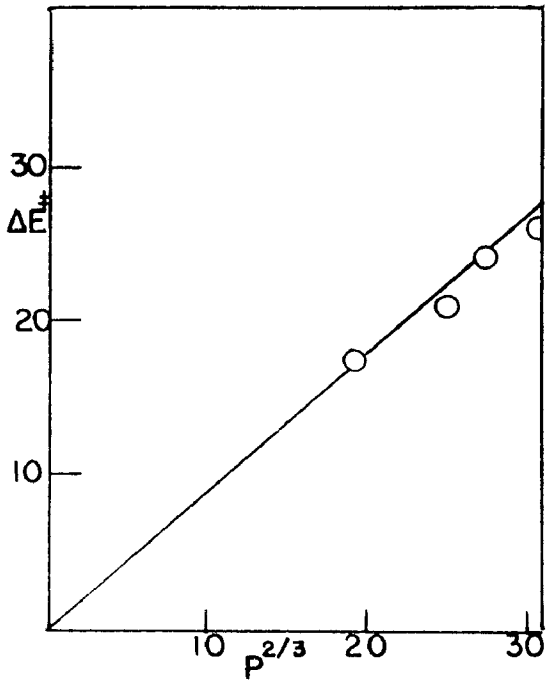

FIGURE 17
$\Delta E^{\ddagger}$ vs. $P^{2/3}$
POLYSTYRENE

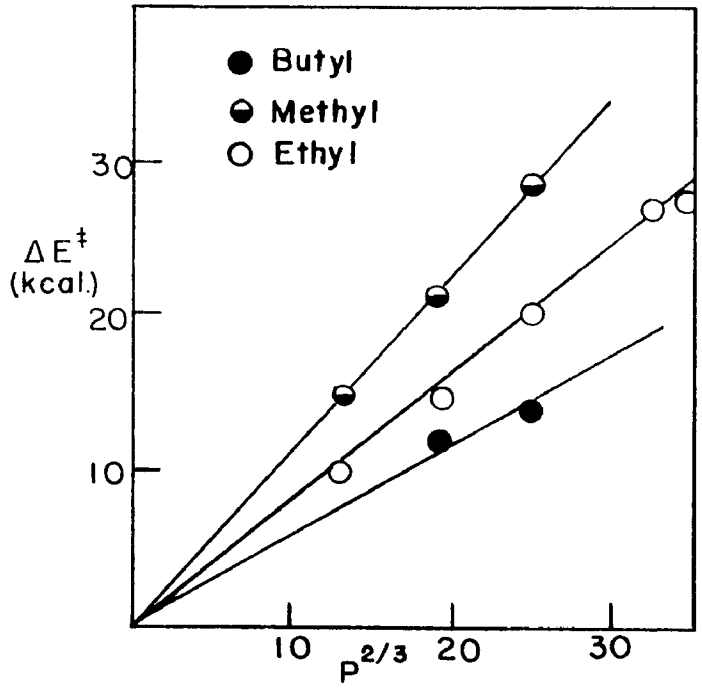

FIGURE 18
$\Delta E^{\ddagger}$ vs. $P^{2/3}$
POLYMERS OF METHYL, ETHYL
AND BUTYL METHACRYLATE

Table 9

Polymer Cohesive Energy Densities

Polymer and Chain Unit	CE/mole of Units	Unit Mol. Wt.	Polymer Density	CE/cc of Units	CED calculated	CED assigned
1. Vinyl acetate						
$-CH_2-CH-OOCCH_3$	4180	86	1.16[a]	48.6	56.4	77.6*
2. Styrene						
$-CH_2CH-C_6H_6$	4980	102	1.05[b]	48.8	51.1	74*
3. Ethyl methacrylate						
$CH_3-CH-CH-COOC_2H_5$	5540	114	1.11[c]	48.6	54.0	76
4. Methyl acrylate						
$-CH_2-CH-COOCH_3$	4180	86	1.15[d]	48.6	55.9	77
5. Methyl methacrylate						
$CH_3-CH-CH-COOCH_3$	4860	100	1.18[c]	48.6	57.4	78
6. Butyl methacrylate						
$CH_3-CH-CH-COOC_4H_9$	6900	142	1.05[c]	48.6	51.0	74

* Ref. 35, experimental values; [a] determined here; [b] Encyclopedia of Chemical Technology; [c] D. E. Strain, R. G. Kennelly, and H. R. Dittmar, Ind. and Eng. Chem. 31 382 (1939); [d] G. Natta and M. Baccaredda, Macrom. Chem. 4 134 (1950).

derived for liquids whose densities are mostly less than unity whereas the seven polymers have densities between 1.05 and 1.18 g/cc, the calculated values for the other four polymers are probably also too low by an equivalent amount. For the purpose of further calculation therefore these four have been assigned values lying in the range between polystyrene and polyvinyl acetate. These are listed in the last column of Table 9 along with the experimental values for polystyrene and polyvinyl acetate.

In choosing molecular cross-sectional areas for hole length calculations the following procedure has been used. First, it was assumed that diffusion cross-sectional area, rather than that from the parachor, controlled hole size for all molecules. Second, in view of the large scatter of points in Figure 14 but the small scatter in Figure 15, the effective cross-sectional areas for the large molecules are probably more accurately fixed by the corresponding values of the diffusion activation energy in polyvinyl acetate rather than by direct determination from gaseous interdiffusion studies. Therefore "true" collision areas for the vapors have been taken as those defined by the line in Figure 14 and the corresponding activation energies. These values were determined for the vapors used with the other five polymers, and are listed in Table 8 also.

Using these values and (17) average hole lengths have been calculated for diffusion in the six polymers and are listed in Table 10. They are seen to lie within a moderately narrow range, bounded by 18 Å. for polybutyl methacrylate and

Table 10

Average Diffusion Hole Lengths and

Polymer Side Group Parachors

Polymer	L	Parachor Large Side Group	Parachor both Groups
Vinyl Acetate	31	98	98
Methyl acrylate	30	98	98
Styrene	25	167	167
Methyl methacrylate	33	98	137
Ethyl methacrylate	23	137	176
Butyl methacrylate	18	215	254

33 Å. for polymethyl methacrylate.

It is of interest to compare the diffusion processes under equivalent conditions (i.e., same diffusing specie) in the various polymers. A correlation has already been noted between the parachor of the side group attached to the chain and the diffusivity for diffusion of hydrogen and water vapor in a variety of polymers, the diffusivity increasing with the parachor.[30] Two alternatives exist here: one is to plot the diffusion activation energy per unit cross-sectional area against some function of the parachor, the other is to plot this quantity normalized in terms of the cohesive energy density (i.e., plot the hole length) against some function of the parachor. The latter course has been chosen although it makes little difference which choice is made since the cohesive energy densities for the six polymers differ by 6% at most. Side group parachors, listed in Table 10, were calculated relative to hydrogen as zero (i.e., the polyethylene chain is taken as the comparison base). Atomic parachors[27] were used for the calculations. Hole lengths are plotted against the parachor of the side group (or the sum of the parachors of the two side groups in the cases of the methacrylates) in Figure 19. A correlation appears to exist, the length decreasing with size of the pendant group.

It should be stated at this point that although a relationship is evident here, the scatter of points does not permit pin-pointing its exact form. One may plot activation energy per unit diffusion cross-sectional area instead of hole length against some function of the parachor. And the

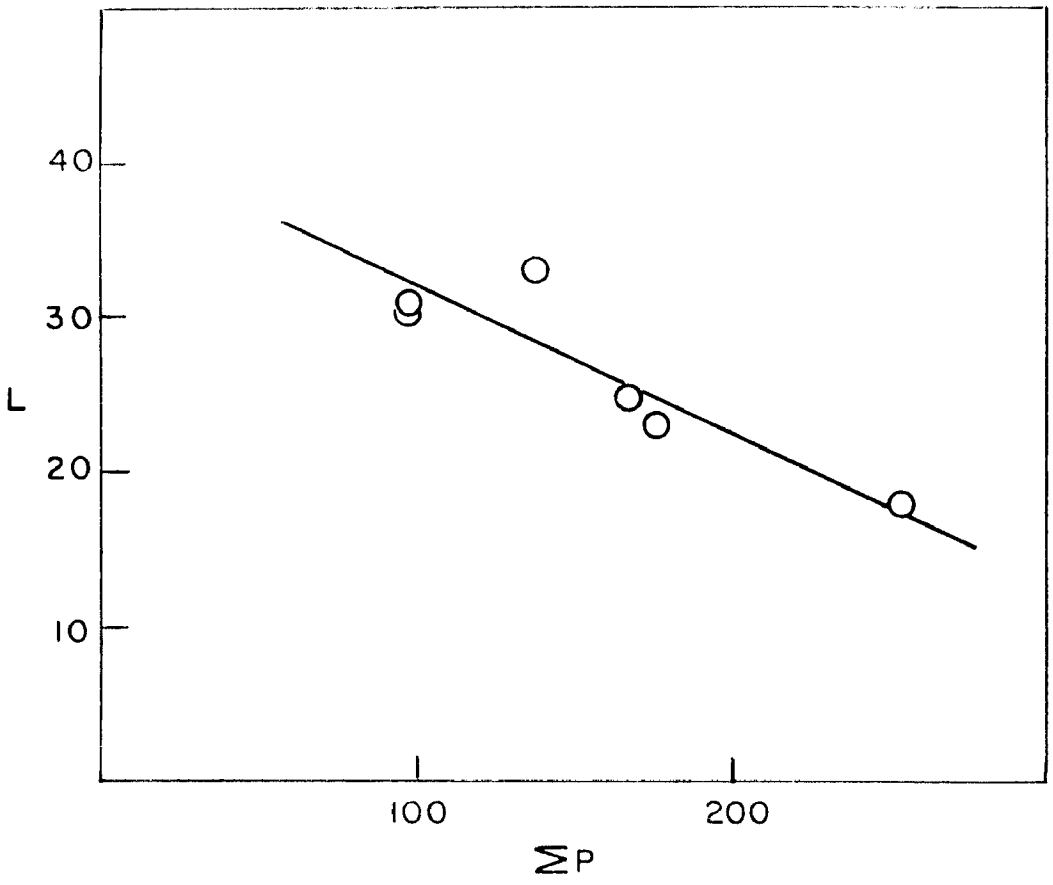

FIGURE 19
L vs. PARACHOR OF BOTH SIDE GROUPS

function may be the parachor of the large side group, the sum for both groups (as in Figure 19) or the two-thirds power of either of these alternatives. (This last was tried in light of the success in correlating activation energies for different vapors in the same polymer by this means.) The scatter is such that no one combination appears much better than any other.

It is interesting to note however that, not only is this relation harmonious with the increase in diffusion coefficients with pendant group parachor noted elsewhere,[30] but also the pendant group size in the latter study varies between zero (polyethylene) and the sizes encountered here so that the appearance of activation data for this work may be useful in extending the sort of correlation discussed here.

It is also of interest to compare the effect of increasing side group size with the effect of introduction of sorbed vapor on the diffusion process. It has already been noted (page 47) that both activation energy and entropy appear to decrease in a roughly linear fashion with increase of vapor concentration, when this change causes an increase in the free volume fraction of the diffusion matrix. In the case of the polymer chain side group, size increase has been seen to produce similar changes in both activation parameters also. (Figure 18 shows ΔE^* to do so and in the next section but one it will be shown that $T\Delta S^*$ is proportional to and smaller than ΔE^*). Such a size increase probably increases the polymer free volume fraction through a decrease in packing efficiency.

The probability that the introduction of a vapor such as ethyl bromide effects the diffusion zone in roughly the same way as an increase in side group size, is strengthened by the fact that a plot of ΔS^* vs $\Delta E^{\ddagger}/T$ for the different concentrations of ethyl bromide yields essentially the same slope as in Figure 20. In summary, it is probably correct to conclude that, in terms of the zone theory, the primary effect in these cases is to lower the average zone size.

Limitations of the Model to Linear Amorphous Polymers

As an illustration of the limitation to linear amorphous polymers of the methods and correlations used above, the behavior of polyethylene will now be discussed. Table 11 lists activation energies for the diffusion of several gases in Grex polyethylene, a non-cross-linked polymer which is 80% crystalline. These were estimated from published data in graphical form. The amorphous regions of polyethylene are well above the glass transition[1] at room temperature so that, except for the crystallinity, this polymer is expected to be like the linear amorphous polymers discussed so far in its diffusion characteristics. However a graph of activation energy vs. collision cross-sectional area does not show the linear relationship found with the six polymers discussed so far. Nevertheless the usual calculation of hole length has been performed, using a value of 64 cal/ml for the cohesive energy density of polyethylene[32] and the results are listed

Table 11

Activation Energies and Apparent Hole Lengths for Diffusion of Gases in Grex Polyethylene

Gas	CSA ($\AA^2$)	$\Delta E^{\ddagger}$ (kcal/mole)	L ($\AA$)
He	3.73	2.12	14.7
O_2	10.3	3.76	9.5
N_2	11.1	4.07	9.5
CO_2	15.1	3.76	6.3

in Table 11 also. The results range from 6 Å for carbon dioxide to 15 Å for helium, a very large percentage spread compared to that found in polyvinyl acetate for example. Furthermore, extrapolation of Figure 19 to zero parachor leads to the prediction that hole lengths of perhaps 40 Å should occur in amorphous polyethylene.

The discrepancies here are at least partially explainable on the basis of the crystallinity of the polymer. It has been estimated from sorption data that the average length of polymer chain between crystalline regions in polyethylene which is 60% crystalline is 15 ± 4 methylene units, corresponding to a maximum average distance between crystallites of about 20 Å.[32] Since diffusion takes place only in the amorphous regions, this means that the upper limit on hole length is 20 Å here, and less than that in the 80%-crystalline polymer. In addition, since the polymer chains are "tied down" at each end (where they enter the crystalline regions), it is not surprising that hole length varies with its width.

Activation Entropies for Diffusion

Having values for activation energy and hole length, and assuming that hole length and path length are identical, the calculation of activation entropy by (14) is possible. Meares found that a plot of activation entropy so calculated versus activation energy for diffusion of the gases in polyvinyl acetate was linear, a type of relationship which had been found to exist for other types of rate processes.[19] In addition it has been recently noted[33] that for diffusion of

water and organic vapors in the six polymers under discussion here the ratio of the activation entropy to activation energy is roughly constant, varying between 1.6 and 2.2 x 10^{-3} deg^{-1}, depending on the polymer. A slight trend to higher ratios with increase in molecular size was noted for polyvinyl acetate but its reality was questioned.

In Tables 6 and 7 are listed activation entropies calculated from Meares' and Ryskin's data using the path lengths calculated herein. In these calculations temperature enters; for Meares' data 27°C. was used in accord with his calculation and for Ryskin's polyvinyl acetate data 55°C. was used since his activation energies were calculated for that temperature. For the rest, no temperatures were listed for the activation energies calculated. Therefore temperatures 30° higher than the glass temperatures of the polymers have been arbitrarily chosen for use in the calculations in light of the fact that 55°C. is 30° higher than the polyvinyl acetate glass temperature.

Following Barrer's procedure,[19] which yields better correlations, activation entropies are plotted against activation energies divided by the absolute temperatures in Figure 20. The data for the vapor diffusion all seem to fit a single straight line while the rare gas data for polyvinyl acetate fit another line, parallel to the first but of lower intercept. The reason for the separate gas line is not known but probably lies either in the difference between ambient temperatures of Meares' and Ryskin's work on polyvinyl acetate, or in

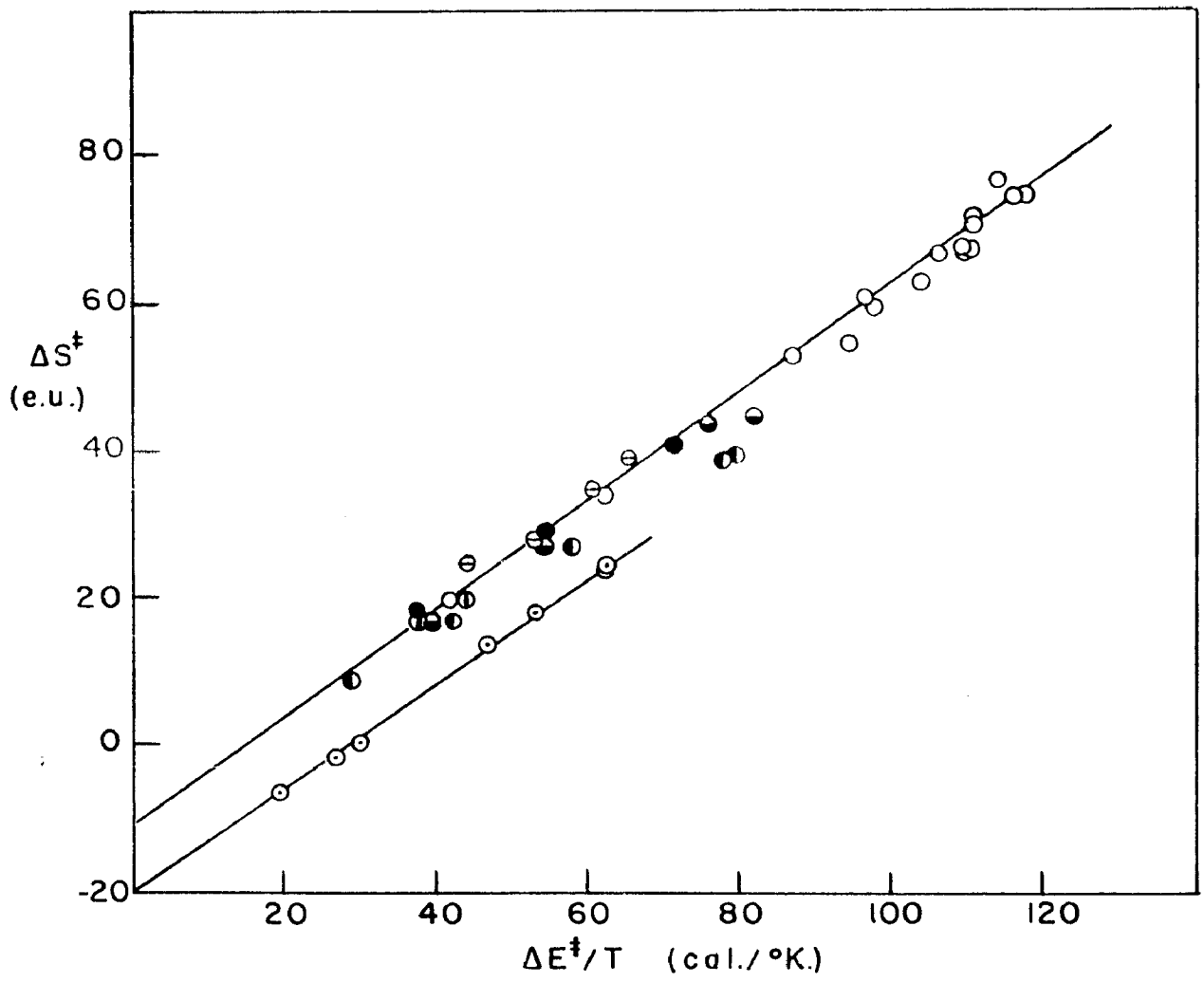

FIGURE 20

$\Delta S^{\ddagger}$ vs. $\Delta E^{\ddagger}/T$
DIFFUSION IN SIX POLYMERS

- ⊙ Polyvinyl Acetate (Gases)
- ○ Polyvinyl Acetate (Vapors)
- ⊖ Polystyrene
- ◒ Polymethyl Acrylate
- ● Polymethyl Methacrylate
- ◐ Polyethyl Methacrylate
- ◑ Polybutyl Methacrylate

the fact that Meares used the time lag method of measurement whereas Ryskin's data were taken by the sorption method. Some such explanation is likely because of the correlation of the higher line of so much data for so many polymers.

The equations for the two lines are

$$\Delta S^{\ddagger} = -11 + 0.73\ \Delta E^{\ddagger}/T \qquad (23)$$

and

$$\Delta S^{\ddagger} = -20 + 0.64\ \Delta E^{\ddagger}/T \qquad (24)$$

These equations are to be compared with

$$\Delta S^{\ddagger} = -4.6 + 0.65\ \Delta E^{\ddagger}/T \qquad (25)$$

which Barrer gives for diffusion in elastomers. The difference in slopes is probably not significant. The negative residual entropies can be understood in terms of the zone theory of diffusion.[19] The unit diffusion step in the substances under discussion seems to require the activation of considerable volume or zone surrounding the diffusion path, as evidenced by the high activation energies encountered and the absence of bond breakage. The loosening up of the polymer element is accompanied by an entropy of disordering (positive), but since the activation energy must be distributed in one of a limited number of ways in order to produce a fruitful loosening, a negative entropy term associated with this restricted distribution is introduced. In addition, a second type of ordering is required; not only must each bond or group have the proper energy in excess of the thermal energy, but the movement of all the segments must be synchronized in order for the hole to open. Now a particle of zero size requires

a hole of zero size and the activation energy is correspondingly nill. That is, diffusion of the hypothetical zero-size particle requires no structural loosening but requires the existence of average conditions in the zone. The energy of the zone must be the average thermal energy and this restriction produces a negative entropy term. In addition this average thermal energy must be distributed properly over the degrees of freedom of the zone. These two ordering processes may spawn decreases in entropy great enough to account for the experimental values.

The greater negative residual entropy for diffusion in the linear polymers compared to that for elastomers can perhaps be partially attributed to a difference in average zone sizes. Diffusion path lengths in rubbers are estimated[19] at 5-10 A; if so, zone sizes might be considerably smaller than those in the linear polymers.

The Temperature Dependence of Activation Energy

Ryskin[25] measured rates of diffusion in a number of instances over wide temperature ranges. Table 12 lists activation energies for methanol, ethanol, and benzene in polyvinyl acetate for temperatures up to 155°C. Those for ethanol were the published values; those for methanol and benzene were estimated here from a graph of log D vs 1/T in the paper and are thus subject to some error. Figure 21 is a plot of activation energy per unit cross-sectional area of the vapor molecule against temperature for these data. Also included

Table 12

Temperature Dependence of Diffusion Activation Energies in Polyvinyl Acetate

	Average T (°C)	$\Delta E^{\ddagger}$ (kcal/mole)
Ethanol		
(Ryskin: Table 11)	85	20.0
	100	23.0
	135	13.8
Benzene		
(estimated from Ryskin graph)	55	38
	105	27
	135	21
	155	15
Methanol		
(estimated from Ryskin graph)	45	18
	75	17
	110	14
	130	12

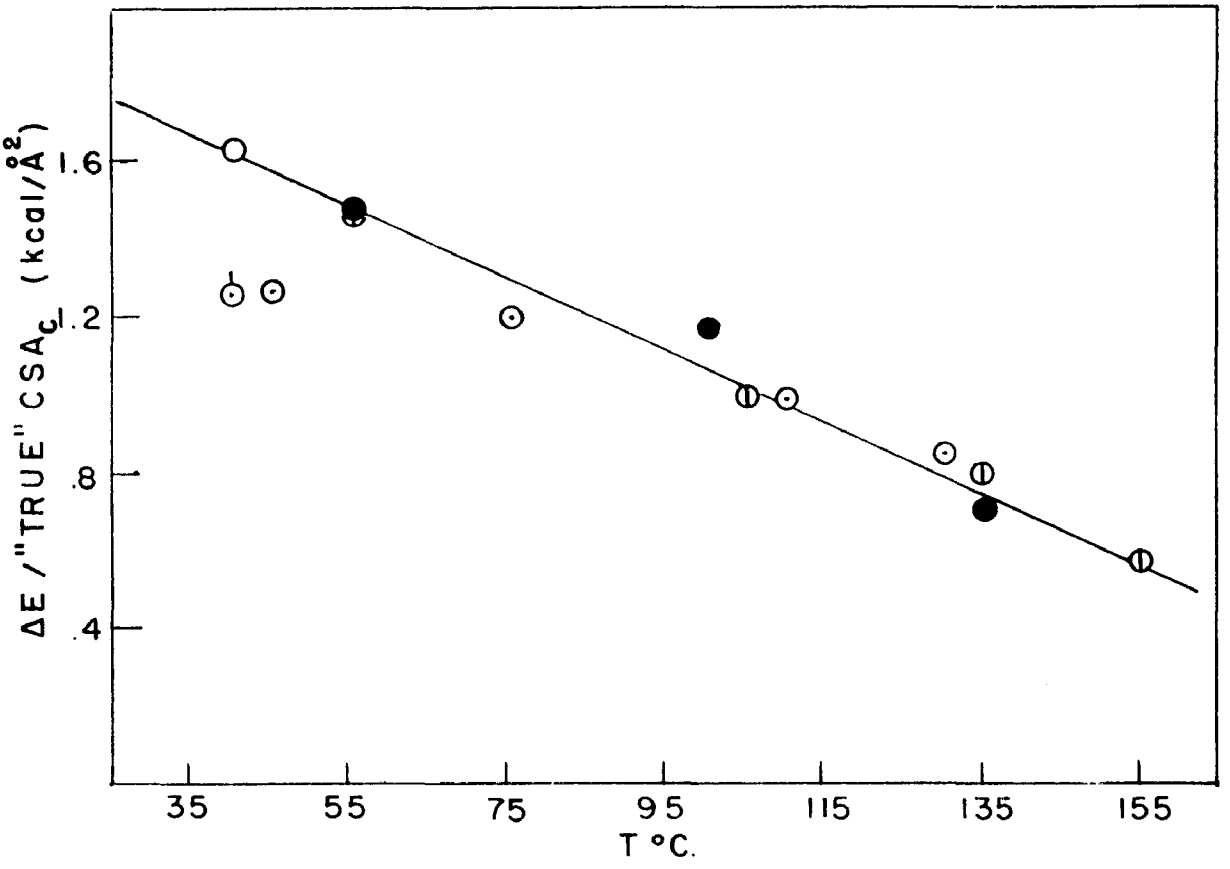

FIGURE 21

$\Delta E^{\ddagger}$ / "TRUE" CSA_c vs. T
DIFFUSION IN POLYVINYL ACETATE

○ C_2H_5Br (this work)
● C_2H_5OH
◐ C_6H_6
⊙ CH_3OH
⊙ CH_3OH (Long[4])

is the point for ethyl bromide at 40° (this work). Finally, a value for methanol at 40° taken from Long's work is graphed for comparison.

A roughly linear increase in activation energy with decrease in temperature is noted, the change equaling 1.0 kcal/A between 25° and 135°C. On this basis and in view of the general scatter of points the ethyl bromide activation energy at 40° appears in reasonable agreement with the rest of the data.

The fact that the single line appears to correlate the data for the vapors of differing size indicates that the essential feature of the diffusion model - activation energy proportional to hole cross-sectional area - holds over a considerable temperature range, to a first approximation at least. The deviation of the methanol points from the line may very well be due simply to errors in the calculation procedure, which explanation is supported by the fact that the ethanol and benzene points lie together whereas, on the basis of molecular size, ethanol would be likely to fall between the two sets if any deviation from the theory is real.

The following proposed explanation of the drop in activation energy with temperature increase is predicated on the assumption that the methanol deviation is not real, and that activation energy drops linearly with temperature roughly. The drop is explainable on the basis of three phenomena: 1) drop in cohesive energy density, 2) drop in collision diameter 3) effect of the number of degrees of freedom in the zone on the temperature coefficient of activation energy.

First, cohesive energy density is susceptible to change with temperature through specific volume change in the polymer. According to Bunn,[29] molar cohesive energy is related to molar volume by

$$(CE_1 - CE_2)/CE_2 = 1.73\ (V_{M_2} - V_{M_1})/V_{M_1} \qquad (26)$$

for hydrocarbons and probably for other non-ionic substances. A similar equation has been derived here for esters on the basis of the changes in heat of vaporization and specific gravity with temperature for ethyl acetate. Vapor pressure data for the former came from the Handbook of Chemistry and Physics and the International Critical Tables. Heats were calculated by means of the Clausius-Clapeyron equation from -40° to $+90^{\circ}$C. and were found to decrease linearly with temperature, the line slope being -12.1 cal/deg. Densities were calculated from data in the latter source as 0.9602 at -30° and 0.8182 at 90°C. Using this data the following obtains for ethyl acetate:

$$\frac{CE_1 - CE_2}{CE_2} = 1.15\ \frac{V_{M_2} - V_{M_1}}{V_{M_1}} \qquad (27)$$

Equation (29) is dimensionless and therefore is equivalent to

$$\frac{e_1 - e_2}{e_2} = 1.15\ \frac{v_2 - v_1}{v_1} \qquad (28)$$

where e and v are cohesion energies and volumes per gram. On the basis of a cohesive energy density of 77.6 cal/ml and a specific volume of 0.862 ml/g, the cohesive energy per gram

for polyvinyl acetate equals 69.9 calories at 25°C. Using a coefficient of volume expansion α equal to 2.32×10^{-4} deg^{-1} from 0° to 25° and 6.94×10^{-4} deg^{-1} above 25° [34], the specific volume at 135°C. may be calculated using the expression

$$v_2 - v_1 = \alpha v_o (T_2 - T_1) \qquad (29)$$

where v_o is the specific volume at 0°C. (v_o is calculated by setting $v_2 = .862$ ml/g, $T_2 = 25°$, $v_1 = v_o$ and $\alpha = 2.32 \times 10^{-4}$.) At 135°C, $v = .927$ ml/g.

Assuming (28) is applicable to polyvinyl acetate and using the above data, $e_{135°} = 64.3$ cal/g. Therefore the cohesive energy density e/v at 135° is 69.4 cal/ml. Thus $CED_2/CED_1 = 69.4/77.6 = 0.893$ so that there is a drop of about 11% in the cohesive energy density over the 110° temperature rise.

A second cause for activation energy decrease lies in the dependence of collision diameter on temperature. If it is assumed that the dependence is roughly the same for diffusion in condensed phases as in gases, Sutherland's formula[28]

$$\sigma_T^2 = \sigma_\infty^2 (1 + C/T) \qquad (30)$$

may be utilized. Both σ_∞^2 and C are empirical constants, σ_∞ being the "hard core" diameter of the molecule, and C also depending on molecular size. Unfortunately few data are available for large molecules and the use of methyl chloride as a representative one has been necessitated. Using C =

454,[28] $T_1 = 298^{\circ}K$ and $T_2 = 408^{\circ}K$, $\left(\frac{408}{298}\right)^2 = 0.84$. That is, there appears to be a 15 - 20% drop in collision cross-sectional areas for organic molecules over the temperature range 25 to 135°C. This will effect a corresponding decrease in activation energy.

If the two contribution discussed so far are combined it is seen that a decrease in activation energy of roughly 25% (or .44 kcal/A^2) over the 110° range is predicted since

$$\frac{E_2}{E_1} = \frac{(CED_2)(CSA_2)}{(CED_1)(CSA_1)} = (.84)(.89) = .75 \qquad (31)$$

assuming L is constant. There remains a further drop of 33% (or .58 kcal/A^2) to be explained.

It will be arbitrarily assumed now that this residual drop can be accounted for solely in terms of the zone theory of diffusion. According to Barrer[19] the decrease in activation energy with temperature, after compensating for changes in hole size etc., is related to the number of activated degrees of freedom f in the zone by

$$\partial \Delta E^{\ddagger} / \partial T = -(f - 1)R \qquad (32)$$

as long as f is large.

On a per-angstrom basis, E / T is therefore assumed to be equal to the .58 kcal/$\mathring{A}^2$ drop divided by 110°; that is $\partial \Delta E^{\ddagger}/\partial T = 5.3$ cal/deg -$\mathring{A}^2$. Using this value (32) becomes

$$f - 1 = 2.7 \text{ per } \mathring{A}^2 \qquad (33)$$

This simplifies to

$$f = 2.7 \text{ per } \mathring{A}^2 \qquad (34)$$

for molecules of even moderate size. For example, for CH_4, using 13 $\mathring{A}^2$ as its cross-sectional area, f from (34) is calculated to be 35. Thus f - 1 is little different from f for CH_4.

This procedure for calculating f gives values in line with corresponding results for diffusion in rubbers. Barrer[19] calculates maximum values of 30 - 40 and minimum values of about 20 for diffusion of CH_4 in various elastomers.

Finally, although the actual magnitudes of f are in doubt due to the uncertainties in the assignment of a value to $\partial \Delta E^{\neq} / \partial T$ in (32), the conclusion that the f is directly proportional to molecular cross-sectional area is probably on safer ground. No change in CED, whether or not it can be calculated correctly from (28) will produce a divergence in activation energy per square angstrom for the different diffusants. Furthermore, since C in (30) has been assumed equal for methanol, ethanol and benzene, a decision that the drop in collision diameter with temperature does not affect $\Delta E^{\neq}$ would simply cause a uniform change in $\partial \Delta E^{\neq} / \partial T$ for all species.

This probable linearity of f with CSA is of great interest. First, it ties in very well with the linearity of hole size and activation energy: the cross-sectional area of the zone is proportional to the cross-sectional area of the hole. Additionally, since the volume of disordered polymer is proportional to hole size, it is natural that the activation entropy be linearly related to activation energy. Finally, the linear dependence of f on CSA appears so far to

be unique for diffusion in condensed systems; calculated values of f for diffusion of hydrocarbons in rubber seem to show no growth trend with increasing molecular size.[42] In view of the similarities in the diffusion behavior of the six polymers notes previously, it seems likely that such linearity of f extends to them and is a characteristic property of linear amorphous polymers as a class. At present there exist insufficient data to test this likelihood.

Uncertainties Concerning the Diffusion Model

Beside the questions caused by the lack of completeness of experimental data such as cohesive energy densities or dependence of activation energy on temperature for the other polymers, there are other, more fundamental uncertainties which arise.

An Alternative to the Use of Cohesive Energy Density.

The first is whether the cohesive energy density is the proper quantity by which to calculate hole volumes. Studies of change in diffusivities with pressure for several inorganic systems has shown that in general for these

$$\Delta V^{*} = 4\beta \Delta H^{\mp} \qquad (35)$$

where ΔV^{*} is the diffusion activation volume and β the isothermal compressibility.[36] The latter quantity has been determined for very few polymers and the former for none.

A third function deserving of attention is the internal pressure P_i defined by

$$P_i = (\partial E/\partial V)_T \approx T\alpha/\beta \qquad (36)$$

where E and α are the internal energy and thermal expansion coefficient, respectively.[37] The approximation is quite good as long as the external pressure is reasonably low. The internal pressure is a measure of the cohesive energy but a simple quantitative relationship appears not to exist.[14] If P_i is the quantity against which the work of hole formation occurs and if this work is essentially equal to the activation energy then

$$\Delta E^{*} = \int_{V_1}^{V_2} (\partial E/\partial V)_T \, dV \qquad (37)$$

where $V_2 - V_1 = \Delta V^{*}$. If P_i is essentially constant over the range of volume expansion encountered in hole formation and if (36) holds in this range then

$$\Delta E^{*} = (\partial E/\partial V)_T \Delta V^{*} = T(\alpha/\beta) \quad V \qquad (38)$$

Extensive studies of both α and β seem to have been undertaken only for polystyrene.[38] The compressibility is 2.20 x 10^{-11} cm^2/dyne at 25°C. and apparently is essentially invariant with temperature. Unfortunately matters are complicated by the existence of two coefficients of expansion - α_1 corresponding to an instantaneous expansion, and α_2 corresponding to the total or equilibrium expansion. Each is actually constant through the glass transition. However, the slow part of the equilibrium expansion, corresponding to $\alpha_2 - \alpha_1$ occurs by an activated rate process with an activation energy of about 12 kcal.[39] The volume change given by $\alpha_2 - \alpha_1$ occurs more and more rapidly with increase in temperature, and from the point of view of macroscopic measurements becomes essential-

ly instantaneous at the glass transition. In the normal methods of determination of expansion coefficients, temperature is raised fast enough to hide completely the slow process up to T_g at which region the slow process becomes fast enough to cause such measurements to yield the equilibrium expansion coefficients. Thus the measured α changes markedly and the temperature at which the change occurs is, by definition, T_g.

If α_1 (= 2.3×10^{-4} °C.$^{-1}$) is the proper coefficient to use in (38), then the activation volume for methanol in polystyrene at 110°C., using $\Delta E^{\ddagger}$ = 17.5 kcal/mole, is calculated from (38) to be 184 cm^3/mole. This compares fairly well with the value of 220 cm^3/mole calculated from the product of L and CSA. On the other hand if α_2 (= 4.3×10^{-4} °C.$^{-1}$) should be used in (38) to calculate activation volumes above T_g then $\Delta V^{\ddagger}$ = 97 cm^3/mole. Finally if (39) is used the activation volume is calculated to be 65 cm^3/mole.

A tentative preference in regard to the two values of activation volume calculated from (38) may be formed by noting that a) activation energy is substantially higher above T_g than it is below generally, and b) the "slow" relaxation process has become rather fast by this point, as evinced by the change in observed α. When the magnitude of the characteristic time for this relaxation decreases to the magnitude of the time length the hole is open, then this process will influence the diffusion mechanism. If this occurs at T_g then α_1 should control diffusion below the transition and α_2 above it. On this assumption activation volumes

$\Delta V_2^{\ddagger}$ and $\Delta V_1^{\ddagger}$ respectively, for diffusion in polystyrene above and below T_g have been calculated from the available data[25] and are listed in Table 13. It was assumed that the activation energies were for $T_g + 30^{\circ}$ and $T_g - 30^{\circ}$ respectively.

Table 13

Diffusion Activation Volumes in Polystyrene Calculated from (40) using α_1 below T_g and α_2 above T_g

Vapor	$\Delta E_2^{\ddagger}$ (kcal)	$\Delta V_2^{\ddagger}$ (ml)	$\Delta E_1^{\ddagger}$ (kcal)	$\Delta V_1^{\ddagger}$ (ml)	$\Delta V_1^{\ddagger}/\Delta V_2^{\ddagger}$
CH_3OH	17.5	98	9.7	118	1.22
C_2H_5CH	21.0	116	9.8	119	1.03
CH_2Cl_2	24.0	132	10	122	.93
C_2H_5Br	26.0	143	12	146	1.02
					Av. = 1.05

From these limited results it appears that hole volumes are roughly equal above and below T_g and that only the mechanisms of volume appregation differ. This equality points to the use of α_2 above T_g as the wiser choice.

An approach similar to this one has been taken by Brandt[40] who has noted the constancy of the ratio $(\alpha_2/\alpha_1)/(\Delta E_2^{\ddagger} / \Delta E_1^{\ddagger})$ at 1.23 to 1.28 for methanol diffusion in polymethyl methacrylate, polyethyl methacrylate, polybutyl methacrylate, and polystyrene. As long as β is constant above and below T_g this ratio is equal to the ratio of hole volumes when these are calculated by (38).

In spite of the apparent success of this model a breakdown occurs when it is applied to molecules of greatly differing size. In Table 14 are listed activation energy ratios for diffusion in polyvinyl acetate calculated from Meares' and Ryskin's data. Using expansion coefficient values[34] of 6.94×10^{-4} °C.$^{-1}$ and 2.32×10^{-4} °C.$^{-1}$ for above and below T_g respectively the listed values for $(\alpha_2/\alpha_1)/(\Delta E_2^*/\Delta E_1^*)$ were calculated. It is seen that the values for the permanent gases scatter about 2.26 but that a sharp drop occurs for the vapors. In light of this the drop in ratio for polystyrene between methanol and the larger molecules now seems significant.

The limitation of this model expresses itself in another way. Whereas a plot of ΔE_1^*, against CSA for the gases is linear[6] in harmony with the linearity of ΔE_2^* vs CSA (Figure 13) the water and methanol points would fall far off the line in contrast to their behavior above T_g.

In summary, the choice of model by which activation volumes, and thus hole lengths, are calculated can still not be made with certainty. For polystyrene L may be 9, 11, 22 or 26 angstroms depending on the model chosen.

<u>Hole Lengths vs Path Lengths.</u> The second uncertainty lies in the calculation of diffusion path lengths. Even if the hole length calculations eventually prove to be correct, there will still be no sound justification for setting equal to L. To say that the average diffusion act requires a hole of certain dimensions does not automatically mean that

Table 14

Activation Volume Ratios for Diffusion in Polyvinyl Acetate above and below T_c

Diffusant	$\Delta E_2^{\neq}$ (kcal)	$\Delta E_1^{\neq}$ (kcal)	$\frac{\Delta E_2^{\neq}}{\Delta E_1^{\neq}}$	$\frac{(\alpha_2/\alpha_1)}{(\Delta E_2^{\neq}/\Delta E_1^{\neq})}$
He	5.35	4.16	1.29	2.32
H_2	7.50	5.17	1.45	2.06
Ne	8.46	7.36	1.15	2.60
O_2	14.49	11.09	1.31	2.28
A	16.50	11.38	1.45	2.06
Kr	19.4	14.5	1.34	2.23
H_2O	13.8	6.4	2.16	1.38
CH_3OH	20.5	7.6	2.70	1.11

the diffusant travels this distance on the average each time. Meares presents arguments for this equality of lengths for the permanent gases; whether or not they are valid for these species, they seem less likely to be so as the molecular size increases.

Future Work

In terms of the diffusion models discussed here, there are several kinds of studies the extensions of which would provide useful information. Examples are listed.

1) Diffusion parameters of the permanent gases in the polymers other than polyvinyl acetate above and below their glass transitions.

2) Experimentally determined values of cohesive energy density for the polymers other than polyvinyl acetate and polystyrene.

3) Diffusion hole length determination in amorphous polyvinyl chloride above its T_g. (Chlorine has a smaller parachor than do any of the side groups of the six polymers discussed here.)

4) Careful determinations of coefficients of expansion and compressibility above and below T_g for the polymers other than polystyrene, and measurements of the rates of the slow relaxation processes below T_g.

The most important kind of measurement is one which has not been done at all up to the present -- The direct de-

termination of activation volumes for gas or vapor limiting diffusivities in polymer systems. The determination of $\Delta V^{\ddagger}$ is accomplished by measuring the effect of external pressure increase on diffusion rate; the relevant equation, analogous to the Arrhenius equation for activation energy, is[22]

$$\partial \ln D / \partial P = - \Delta V^{\ddagger} / RT \qquad (39)$$

Such studies would be experimentally difficult but the results would be extremely rewarding in terms of testing the various models discussed here in an unequivocal fashion.

SUMMARY

V. SUMMARY

Diffusion coefficients from rates of sorption, and equilibrium isotherms, for ethyl bromide at 30°, 40°, and 50° C. in polyvinyl acetate film have been determined with a McBain balance. The heat of mixing is zero and its significance is discussed in terms of the Scatchard-Hildebrand rule and the isotherms for other vapors in the polymer. The limiting diffusion activation energy is determined to be 41 kcal/mol at 40° C. which compares well with other published results. The contrast in the effect of ethyl bromide concentration of the diffusion activation parameters, as opposed to that of acetone and benzene is tentatively correlated with differences in free volume fractions of the vapor-polymer systems.

Isotherms at 30° and 40° and diffusivities at 30° have been taken for acetonitrile. Diffusion behavior is roughly as expected. The heat of mixing appears to be zero over most of the concentration range studied in contradiction to the expectation based on the widely differing cohesive energy densities of liquid and polymer. This behavior is discussed in terms of nitrile dipole-pair formation.

An extensive discussion of published data for the diffusivities of gases and vapors in six linear amorphous polymers is presented. It is seen that the diffusion process appears to be essentially the same for all gases and all vapors in all linear amorphous polymers above their glass temperatures. Although many details of the mechanism of

limiting diffusion still are uncertain the following may be stated for the polymer class as a whole with some certainty.

1) Activation energies and entropies are linearly dependent on diffusant cross-sectional areas for all gases and vapors.

2) Activation parameters are independent of all other properties of the diffusant (as long as the sorption is not chemisorption).

3) Activation parameters for diffusion of a particular impurity decrease linearly with increase in size of the polymer chain side group. Furthermore a characteristic quantity L for each polymer may be determined which has linear dimensions, is roughly constant for diffusion of any molecule in the given polymer, and appears to be a decreasing linear function of the polymer chain side group size. It is probably proportional to the length of the diffusion hole and may even equal it.

4) The number of activated degrees of freedom in the diffusion zone are directly proportional to diffusant cross-sectional area in polyvinyl acetate, in harmony with 1). It is likely that this is true for the other polymers but the data for testing this are not available.

In regard to these simple diffusion behavior characteristics, linear amorphous polymers, above their glass temperatures at least, appear to form a unique class of high polymers.

TABLES OF KINETIC DATA

TABLES OF KINETIC DATA

Ethyl Bromide

I. Runs #10, 11, 12, and 14 at 30°C.

1. P/P_o = .0721, W = .0220
ℓ = .000422 cm

$\Delta W/\Delta W_\infty$	t (min.)
.047	25
.144	60
.332	130
.382	190
.476	250
.523	310
.523	370
.609	445
.570	510
.810	1625
.866	2025
1	2300
1	2880
.952	2915
.070	2
.070	4
.070	10
.25	20
.17	30
.39	60
.39	90
.43	120
1.05	660
1.0	970

2. P/P_o = .136, W_e = .0390
ℓ = .000422

$\Delta W/\Delta W_\infty$	t (min.)
.07	1
.106	4
.106	7
.214	15
.284	25
.355	32
.464	55
.499	65
.0220	75
.0195	90
.0183	110
.0183	135
.0158	165
.0124	245
.0098	375
.0085	515
.0073	735
.0037	1410
.0049	1545
.0049	1705
.0037	3165
.0049	4500

3. P/P_o = .171, W = .0480
ℓ = .000422 cm

$\Delta W/\Delta W_\infty$	t (min.)
0	1
.025	2
.025	2.5
.050	3
.025	3.5
.025	4
.050	5
.075	6
.075	7
.075	8
.127	10
.127	11
.127	12
.127	13
.152	15
.202	18
.229	19.5
.229	21
.229	22
.229	25
.304	27.5
.331	28.5

$\Delta W/\Delta W_\infty$	t(min.)
.681	33.5
.725	39
.770	45
.802	50
.835	55
.845	60
.879	70
.967	135
.989	230
1.0	285
.112	0.5
.0786	1.0
.067	1.5
.090	2.0
.102	2.5
.113	3.0
.157	4.0
.168	5.0
.191	6.0
.202	7.0
.225	8.0
.236	9.0
.247	10
.258	11
.270	12
.292	13
.303	14
.326	16
.360	19
.370	21
.382	23
.415	27
.438	30
.472	38
.528	49
.573	62
.595	71

4. P/P_o = .0649, W = .0167

$\Delta W/\Delta W_\infty$	t (min.)
.059	1
.088	2
.118	3
.118	4
.176	5
.176	6
.176	8
.206	10
.265	14

$\Delta W/\Delta W_\infty$	t (min.)
.324	18
.353	23
.382	28
.441	35
.500	47
.530	62
.647	100
.794	150
.823	170
.832	265
.912	390
.941	495
1	1400
.086	0.75
.052	1.25
.052	1.75
.029	2.5
.052	3.0
.052	4.5
.085	6.0
.115	8.0
.172	17
.201	23
.258	30
.287	38
.344	46
.373	67
.457	88
.486	114
.514	139
.572	170
.686	265
.715	330
.743	360

5. P/P_o = .213, W = .0628

$\Delta W/\Delta W_\infty$	t (min.))
.125	1.25
.187	1.75
.211	2.25
.266	3.0
.320	4.0
.375	5.0
.422	6.25
.453	7.0
.485	8.0
.523	9.0
.547	10
.570	11
.586	12

2. P/P_o = .127, W = .0363

$\Delta W/\Delta W_\infty$	t (min.)
0	0.5
.081	1.0
.095	1.5
.122	2.0
.135	2.5
.149	3.0
.162	3.5
.176	4.0
.189	4.5
.203	5.0
.189	6.0
.203	7.0
.244	8
.270	9
.270	10
.297	11
.311	12
.324	13
.338	14
.365	15
.378	16
.378	17
.406	19
.432	21
.446	23
.473	26
.500	30
.541	34
.568	38
.610	42
.635	46
.649	50
.675	55
.690	60
.716	65.5
.744	70.5
.757	75
.770	80
.797	90
.838	105
.865	120
1.0	830
1.0	1070
.103	0.5
.051	1.0
.064	1.5
.064	2.0
.077	2.5
.090	3.0
.103	4.0
.115	5
.154	7
.179	9
.205	11
.231	13
.244	15
.256	17
.282	20
.295	24
.333	30
.372	35
.398	40
.436	49
.513	72
.615	93
.667	120
.757	195

3. P/P_o = .157, W = .0447

$\Delta W/\Delta W_\infty$	t (min.)
.077	1.0
.121	1.5
.143	2.0
.165	2.5
.187	3.0
.209	3.5
.242	4.5
.264	5.0
.275	5.5
.286	6.0
.319	7.0
.330	7.5
.341	8.0
.341	8.5
.363	9
.385	10
.407	11
.428	12
.430	13
.462	14
.483	15
.495	16
.505	17
.528	19
.560	21
.571	22
.583	24
.627	27
.660	30

$\Delta W/\Delta W_\infty$	t (min.)
1.0	1185
.068	1.0
.054	1.5
.068	2.0
.068	2.5
.081	3.0
.095	7.0
.122	10.0
.122	13
.135	16
.149	20
.175	25
.189	30
.216	36
.230	47
.243	59
.284	73
.297	87
.324	105
.348	141
.405	197
.307	18
.326	20
.346	23.5
.384	26
.404	29
.423	33
.467	38.5
.577	60
.692	63
.731	109
.865	190
.885	225
.942	285
.962	370
1.0	520
1.0	1110

II. Run #13 at 40°C.
ℓ = .000825

1. P/P_o = .0949, W = .0255

$\Delta W/\Delta W_\infty$	t (min.)
.038	1.16
.058	1.5
.058	2.0
.058	2.5
.066	3.0
.115	3.67
.137	4.0
.135	4.5
.135	5.0
.135	5.5
.154	6.0
.173	6.5
.173	7.0
.192	8.0
.211	9
.211	10
.231	11
.269	12
.269	13
.269	14
.269	15
.269	16
.184	0.5
.143	1.0
.061	1.5
.041	2.0
.061	2.5
.082	3.0
.082	3.5
.102	4.0
.102	4.5
.102	5
.122	6
.102	7
.143	8
.163	9
.184	10
.184	11
.204	12
.225	14
.245	17
.286	21
.306	24
.347	29
.368	35
.408	40
.490	60
.510	70
.592	90
.592	106
.592	120
.694	225
.837	445
.939	1045
1.0	1225
1.0	1535

$\Delta W/\Delta W_\infty$	t (min.)
0	1.16
.024	2
.032	2.5
.049	3
.056	4
.081	5
.097	6
.121	7
.129	8
.137	9
.153	10
.161	11
.177	12
.185	13
.201	14
.210	15
.218	16
.226	17
.234	18
.250	20
.274	22
.298	24
.306	26
.322	28
.338	30
.355	32
.371	34
.411	40
.427	44
.443	48
.476	53
.500	56
.516	60
.524	65
.548	71
.572	77
.613	87
.637	100
.870	240
.895	280
.919	310
.969	450
1.0	1040
.072	0.5
.048	1.0
.040	1.5
.065	2.0
.065	2.5
.065	3.0
.081	3.5
.081	4.0
.089	5.0
.105	6
.105	7
.121	8
.137	11
.145	13
.169	15
.169	18
.194	22
.210	25
.234	30
.258	35
.274	40
.288	45
.329	60
.352	72
.385	89

7. P/P_o = .136, W .0363
ℓ = .000825 cm

$\Delta W/\Delta W_\infty$	t (min.)
0	1
0	2
0	3
.010	7
.027	10
.068	16
.122	26
.189	44
.230	54
.257	63
.311	84
.351	95
.365	106
.378	116
.405	128
.432	145
.459	156
.487	171
.513	190
.527	205
.554	219
.675	315
.743	380
.784	418
.824	520
.705	660

$\Delta W/\Delta W_\infty$	t (min.)
.665	24.5
.675	25
.680	25.5
.685	26
.685	26.5
.690	27
.700	28
.710	29
.720	30
.770	34.5
.780	35
.785	36
.805	38
.820	39
.825	40
.835	41
.840	42
.860	46
.880	49
.890	51
.910	54
.920	56
.925	58
.930	60
.940	63
.950	67
.955	74
.970	82
.980	87
.990	100
.985	105
.995	195
1.00	330

.065	.67
.075	1.0
.105	1.5
.115	2.0
.130	2.5
.145	3.0
.155	3.33
.160	3.67
.175	4.0
.185	4.33
.190	4.67
.190	5.0
.205	5.33
.212	5.67
.212	6.0
.221	6.33
.226	6.67
.231	7.0
.240	7.5

$\Delta W/\Delta W_\infty$	t (min.)
.245	8.0
.250	8.5
.265	9.0
.274	10.0
.288	11
.298	12
.308	13
.317	14
.327	15
.336	16
.351	17
.361	19
.361	20
.365	21
.370	22
.380	24
.390	26
.400	27
.405	28
.410	29
.410	30
.435	36
.455	42
.480	50
.495	54
.500	57
.510	64
.520	69
.540	79
.560	89
.575	102
.580	110
.600	126
.615	141
.630	152
.635	169
.655	189
.665	201
.685	233
.705	290
.715	330
.730	370
.836	955
.855	1195
.865	1370
.915	2270

6. $P/P_o = .206$, $W = .0608$
   $\ell = .000825$ cm

$\Delta W/\Delta W_\infty$	t (min.)
.865	39
.841	41
.873	43
.889	45
.905	47
.920	48
.968	55
.984	60
1.0	65
.984	70
1.0	80
1.0	90
.175	.41
.175	1
.143	2
.175	3
.206	4
.238	5
.270	6
.286	7
.302	8
.318	9
.365	11
.381	12
.381	13
.397	14
.397	15
.428	18
.445	19
.445	21
.460	22
.482	25
.482	28
.508	29
.524	31
.540	33
.540	35
.555	37
.571	41
.571	45
.698	73
.730	105
.761	135
.810	175
.825	205
1.0	770

5. P/P_o = .310, W = .1020
ℓ = .000825 cm

$\Delta W/\Delta W_\infty$	t (min.)
.029	1.08
.063	1.75
.091	2.25
.106	2.67
.135	3.25
.159	3.5
.163	4.0
.178	4.33
.183	4.67
.192	5.0
.202	5.33
.231	6.0
.240	6.33
.255	6.67
.260	7.0
.274	7.33
.293	7.67
.298	8.0
.317	8.5
.332	9.0
.351	9.5
.365	10.0
.380	10.5
.394	11.0
.418	12.0
.433	12.5
.447	13.0
.457	13.5
.465	14.0
.475	14.5
.485	15.0
.510	16.0
.525	16.5
.530	17.0
.555	18
.577	19
.580	19.5
.590	20
.595	20.5
.605	21
.615	21.5
.625	22
.630	22.5
.640	23
.650	23.5
.655	24

$\Delta W/\Delta W_\infty$	t (min.)
.331	29.5
.331	30
.331	31
.356	32
.381	33
.406	34
.406	35
.431	36
.431	37.5
.431	39
.459	41
.459	43
.483	45
.483	49
.508	54
.583	60
.609	64
.635	68
.660	74
.712	78
.735	86
.762	90
.807	97
.838	104
.864	115
.888	120
.915	129
.940	145
.964	151
.964	160
1.0	170
1.0	765

.07	2
.14	3
.11	4
.11	5
.14	6
.14	7
.17	8
.20	9
.17	10
.24	11
.268	12
.24	13
.268	14
.299	15
.268	16
.299	17
.299	18
.330	19

$\Delta W/\Delta W_\infty$	t (min.)
.330	20
.396	24
.427	28
.458	33
.490	37
.524	45
.618	70
.681	85
.875	160
.938	255
1.0	450
1.0	525
1.0	2900

4. P/P_o = .248, W = .0768
ℓ = .000422 cm

$\Delta W/\Delta W_\infty$	t (min.)
0	1
.067	1.5
.083	2
.116	2.5
.133	3
.100	4
.116	4.5
.133	5
.166	6
.216	7.5
.249	8.5
.233	9
.266	9.5
.282	10.5
.282	11
.332	13
.332	14
.399	15
.416	16
.449	17
.449	18
.449	19.5
.532	21
.565	22
.582	23
.598	24
.632	25
.665	27
.698	29
.698	31
.815	36
.831	38

$\Delta W/\Delta W_\infty$	t (min.)
.610	13
.649	14
.672	15
.688	16
.695	17
.743	18
.743	19
.774	20
.781	21
.789	22
.797	23
.805	24
.813	25
.820	26
.828	27
.852	29
.860	31
.875	33
.891	37
.898	40
.930	48
.109	0.5
.101	1.0
.109	1.5
.141	2.0
,156	2.5
.180	3.0
.203	3.5
.219	4.0
.234	4.5
.242	5
.266	6
.289	7
.305	8
.328	9
.344	10
.359	11
.375	12
.390	13
.406	14
.414	15
.437	17
.453	19
.476	21
.492	23
.508	25
.524	28
.540	30
.586	37
.602	46
.680	69
.945	909
.953	1040

III. Run #15 at 50°C
ℓ = .000667 cm

1. P/P_o = .0549, W = .0154

$\Delta W/\Delta W_\infty$	t (min)
.098	1.0
.195	1.5
.244	2.0
.292	2.5
.317	3.0
.342	3.5
.390	4.0
.415	4.5
.439	5.0
.488	6
.537	7
.585	8
.635	9
.659	10
.708	11
.708	12
.708	13
.756	15
.781	16
.805	17
.805	18
.830	19
.854	20
.878	22
.878	24
.903	26
.976	30
.952	35
.976	40
1.0	50
1.0	60
.462	0.33
.205	1.0
.205	1.33
.231	1.67
.231	2.5
.282	3.0
.256	3.5
.308	4.0
.384	5.33

$\Delta W/\Delta W_\infty$	t (min.)
.384	6.0
.410	6.5
.410	7.0
.436	8
.487	9
.512	10
.538	11
.590	12
.590	13
.615	14
.641	16
.692	18
.718	20
.743	22
.743	24
.769	25
.769	27
.820	30
.795	35
.821	40
.888	50
.975	150
1.0	240

2. $P/P_o = .761$, $W = .0218$

$\Delta W/\Delta W_\infty$	t (min.)
.172	0.75
.241	1.16
.293	1.50
.328	1.75
.345	2.08
.362	2.50
.413	3.0
.448	3.33
.465	3.67
.483	4.0
.500	4.33
.517	4.67
.535	5.0
.552	5.33
.569	5.67
.587	6.0
.603	6.5
.621	7.0
.655	7.5
.672	8.0
.690	8.5
.706	9.0
.724	9.5
.741	10
.775	11
.810	12
.793	13
.826	14
.845	15
.879	17
.896	19
.914	21
.930	25
.947	30
.981	40
1.0	55
1.0	70

.264	0.5
.208	1.0
.208	1.5
.245	1.83
.302	2.33
.321	2.67
.340	3.0
.358	3.33
.378	3.67
.396	4.0
.415	4.33
.434	4.67
.453	5.0
.472	5.33
.453	5.67
.491	6.0
.491	6.5
.510	7.0
.529	7.5
.547	8.0
.566	8.5
.585	9.0
.623	10
.641	11
.660	12
.679	13
.698	14
.717	15
.755	17
.782	20
.830	25
.869	30
1.0	120
1.0	1230

3. P/P_o = .0980, W = .0278

$\Delta W/\Delta W_\infty$	t (min.)
.207	1
.276	1.5
.302	1.75
.329	2.0
.356	2.25
.382	2.5
.408	2.75
.434	3.0
.447	3.25
.473	3.50
.487	3.75
.513	4.0
.526	4.25
.540	4.50
.540	4.75
.565	5.0
.592	5.25
.618	5.75
.631	6.0
.645	6.33
.671	6.67
.684	7.0
.696	7.33
.723	8.0
.736	8.5
.736	9.0
.763	9.5
.776	10.0
.790	10.5
.803	11
.828	12
.855	13
.868	14
.895	16
.907	18
.934	21
.947	25
.960	33
1.0	125

W/ W	t (min.))
.243	1.33
.297	2.0
.311	2.5
.433	3.25
.432	4.25
.460	5.0
.487	5.5
.500	6.0
.513	6.5
.527	7.0
.541	7.5
.554	8.0
.568	8.5
.595	9.0
.608	9.5
.622	10.0
.635	10.5
.649	11.0
.663	11.5
.675	12.0
.690	13
.716	15
.757	17
.825	23
.852	26
.879	30
.945	60
.973	125

4. P/P_o = .121, W = .0353

$\Delta W/\Delta W_\infty$	t (min.)
.234	1.22
.277	1.37
.298	1.50
.319	1.65
.341	1.77
.362	1.90
.383	2.07
.394	2.18
.415	2.30
.426	2.45
.447	2.60
.458	2.72
.479	2.85
.490	3.08
.511	3.28
.532	3.40
.553	3.53
.564	3.70
.564	3.85
.585	4.0
.596	4.12
.606	4.27
.617	4.38
.628	4.50
.638	4.60
.638	4.78
.650	4.90
.671	5.07
.692	5.50

$\Delta W/\Delta W_\infty$	t (min.)
.702	5.78
.723	6.03
.735	6.22
.745	6.35
.745	6.55
.766	6.93
.841	8.50
.851	9.15
.883	11
.894	12
.904	13
.926	16
.947	21
.968	32
1.0	120

$\Delta W/\Delta W_\infty$	t (min.)
.691	12.5
.765	18
.787	20
.819	23
.830	26
.851	29
.893	38
.915	50
.979	115

.[illegible]	0.40
.234	0.60
.223	0.82
.234	1.03
.245	1.18
.255	1.38
.277	1.55
.287	1.68
.298	1.85
.319	1.98
.319	2.13
.340	2.35
.351	2.50
.362	2.67
.383	2.92
.394	3.10
.404	3.25
.404	3.37
.415	3.55
.426	3.70
.436	3.90
.457	4.12
.468	4.33
.479	4.54
.489	4.85
.500	5.03
.532	5.48
.532	5.70
.543	5.93
.553	6.25
.575	6.48
.585	6.77
.585	6.92
.606	8.75
.649	10

Acetonitrile

Runs #10 – B and #11 – B
T = 30°C ℓ = .000535 cm

1. P/P_o = .0864, W = .0137

$\Delta W / \Delta W_\infty$	t (min.)
.13	5
.33	10
.40	15
.53	22
.60	30
.66	40
.73	55
.80	70
.80	90
1.07	180
.93	240
1.07	300
1.0	375
.30	2
.46	5
.53	8
.61	10
.77	12
.93	14
.93	16
1.00	20
1.00	1560

2. P/P_o = .190, W = .0337

$\Delta W / \Delta W_\infty$	t (min.)
.25	1
.53	2
.75	3.5
.81	4
.86	5
.89	6
.98	7
.98	8
.98	9
1.00	11
1.00	75
.44	1
.64	2
.64	3
.67	4
.69	5
.69	6
.72	7
.78	10
.83	15
.89	25
.92	40
.97	60
.97	130

3. P/P_o = .267, W = .0491

$\Delta W / \Delta W_\infty$	t (min.)
.41	1
.73	2
.89	3
.93	4
.96	5
1.00	7
1.00	10
.98	15
1.00	50
.37	0.5
.56	1.5
.61	2.5
.67	3.5
.68	4
.74	5
.74	6
.78	7
.80	8
.81	10
.87	15
.89	20
.94	55
.98	750

4. P/P_o = .0868, W = .0146

$\Delta W / \Delta W_\infty$	t (min.)
.12	1
.38	2
.38	3
.50	4
.38	5
.56	7
.50	9
.62	11
.69	15
.81	20
.94	25
.94	35
1.00	80
1.00	115
.50	1
.50	2
.66	3
.66	4
.74	6
.83	7
.83	8
.74	9
1.0	10
.92	11
1.0	13
.92	30

5. P/P_o = .119, W = .0209

$\Delta W / \Delta W_\infty$	t (min.)
.08	2
.21	3
.33	4
.37	5
.46	6
.50	7
.54	8
.63	9
.63	10
.67	11
.71	14
.79	15
.83	16
.87	18
.87	20
.87	24
.90	40
1.00	70
1.00	150
.26	1

$\Delta W / \Delta W$	t (min.)
.30	2
.39	3
.48	4
.52	5
.48	6
.52	7
.57	8
.61	10
.65	12
.65	14
.69	16
.74	19
.78	25
.78	30
.73	40
.87	55
.87	75
.92	680

6. P/P_o = .220, W = .0400

$\Delta W / \Delta W$	t (min.)
.22	1
.51	2
.69	3
.84	4
.93	5
.98	6
1.00	8
.98	10
.98	12
1.00	30
.98	45
1.00	105
.48	1
.56	2
.61	3
.72	4
.74	5
.78	6
.78	7
.85	8
.87	10
.89	12
.91	15
.93	20
.98	31
1.00	60

7. P/P_o = .124, W = .0227

$\Delta W / \Delta W_\infty$	t (min.)
.16	.67
.24	1.0
.28	1.25
.32	1.50
.36	1.75
.40	2.0
.40	2.25
.44	2.50
.44	2.75
.44	3.0
.44	3.25
.44	3.50
.44	3.75
.44	4.0
.48	4.25
.48	4.50
.52	5.0
.48	5.5
.52	6.0
.56	7.0
.64	8.0
.64	8.5
.64	9.0
.68	10
.72	11
.76	12
.80	13
.80	14
.88	15
.84	16
.88	17
.88	19
.88	21
.96	26
1.0	30
1.0	455
.16	.33
.16	.75
.20	1.25
.28	1.75
.28	2.00
.32	2.50
.36	2.75
.36	3.0
.36	3.25
.36	3.50
.40	3.75
.40	4.00
.40	4.25
.44	4.50
.40	4.75
.44	5.0
.48	5.50
.48	6.00
.48	6.50
.48	7.00
.48	7.50
.52	8.00
.52	8.50
.52	9.00
.52	11
.56	11
.56	12
.60	13
.60	14
.60	15
.60	17
.64	18
.64	20
.64	22
.68	25
.72	35
.76	63
.76	90
.72	125
.72	255

8. P/P_o = .230, W = .0433

$\Delta W / \Delta W_\infty$	t (min.)
.15	.83
.21	1.0
.25	1.50
.32	1.83
.36	2.08
.46	2.50
.49	2.75
.53	3.0
.60	3.25
.63	3.5
.65	4.0
.77	4.5
.82	5.0
.84	5.25
.86	5.50
.91	5.75
.92	6.0
.95	6.25

$\Delta W / \Delta W_\infty$	t (min.)
.95	6.50
.97	7.0
.95	7.25
.97	7.5
1.00	8.0
1.00	30
.31	.45
.40	1.00
.44	1.33
.48	1.67
.50	2.0
.52	2.33
.54	2.67
.58	3.0
.64	3.67
.64	4.0
.67	4.33
.69	4.67
.71	5.0
.71	5.5
.71	6.0
.77	7
.77	8
.79	9
.81	10
.83	12
.83	15
.85	18
.87	25
.92	35
.96	50

9. P/P_o = .153, W = .0264

$\Delta W / \Delta W_\infty$	t (min.)
.07	.92
.14	1.33
.17	1.67
.24	2.0
.31	2.33
.34	2.67
.34	3.0
.41	3.33
.45	3.67
.48	4.0
.52	4.33
.55	4.67
.55	5.0
.59	5.33
.62	5.67
.62	6.0
.62	6.33
.66	6.67
.69	7.0
.72	7.33
.76	7.67
.76	8.0
.79	8.33
.79	8.67
.83	9.0
.83	9.33
.83	9.67
.86	10.0
.86	10.33
.90	10.67
.90	11.0
.93	11.33
.90	11.67
.93	12.0
.93	12.5
.99	13.0
.99	13.5
.99	14.0
.99	14.5
.97	15.0
.97	15.5
1.00	16
1.00	93
.28	.45
.34	1.00
.38	1.50
.38	1.75
.45	2.00
.41	2.25
.45	2.50
.49	2.75
.55	3.25
.55	3.50
.55	4.0
.59	4.5
.62	5.0
.66	5.5
.66	6.0
.66	6.5
.69	7.0
.72	7.5
.76	8.0
.76	8.5
.76	9.0
.76	10.0
.76	11

$\Delta W / \Delta W_\infty$	t (min.)
.79	12
.86	15
.97	19
.90	22
.93	25
1.00	32

10. P/P_o = .123, W = .0218

$\Delta W / \Delta W_\infty$	t (min.)
.17	1.00
.17	1.25
.21	1.50
.25	1.75
.25	2.0
.21	2.25
.25	2.50
.29	2.75
.29	3.0
.29	3.25
.33	3.50
.33	3.75
.33	4.0
.38	4.25
.42	4.50
.42	4.75
.46	5.0
.46	5.25
.51	5.50
.46	6.0
.51	6.25
.51	6.50
.51	6.5
.51	6.75
.55	7.0
.55	7.5
.60	7.75
.60	8.0
.60	8.25
.60	8.5
.64	8.75
.64	9.0
.64	9.25
.69	9.5
.69	9.75
.69	10.0
.69	10.25
.69	10.5
.69	10.75
.69	11.0
.73	11.75
.78	12.25
.78	13.0
.78	13.5
.78	14
.84	14.5
.84	15
.88	15.5
.88	16
.88	17
.88	18
.92	19
.92	20
.96	21
.96	22
.96	23
1.00	24
1.00	120

$\Delta W / \Delta W_\infty$	t (min.)
.31	.50
.31	.75
.40	1.00
.40	1.25
.40	1.50
.40	1.75
.40	2.00
.50	2.50
.50	2.75
.50	3.0
.54	3.25
.54	3.50
.54	3.75
.54	4.0
.58	4.5
.58	5.0
.62	5.5
.67	6.0
.71	6.5
.67	7.0
.71	8
.71	9
.75	10
.79	11
.84	12
.84	13
.84	14
.84	15
.88	18
.88	20
.92	30
1.00	40

REFERENCES

REFERENCES

1. P. J. Flory, Principles of Polymer Chemistry, Cornell University Press, Ithaca, N. Y., 1953.

2. J. Crank and G. S. Park, Trans. Far. Soc. 45 240 (1949).

3. G. S. Park, Trans. Far. Soc. 46 684 (1950).

4. R. J. Kokes, F. A. Long and J. L. Hoard, J. Chem. Phys. 20 1711 (1952).

5. F. A. Long and R. J. Kokes, J. Am. Chem. Soc. 75 2232 (1953).

6. P. Meares, J. Am. Chem. Soc. 76 3415 (1954).

7. P. Meares, Trans. Far. Soc. 53 1146 (1957).

8. J. Crank and M. E. Henry, Trans. Far. Soc. 45 1119 (1949).

9. R. M. Barrer, Diffusion in and Through Solids, Macmillan Co., New York, N. Y. and Cambridge University Press, Cambridge, England, 1941.

10. R. J. Kokes and F. A. Long, J. Am. Chem. Soc. 75 6142 (1953).

11. S. Prager and F. A. Long, J. Am. Chem. Soc. 73 4072 (1951).

12. J. A. Manson, Air Reduction Co., Private communication.

13. R. J. Kokes, A. R. diPietro and F. A. Long, J. Am. Chem. Soc. 75 6319 (1953).

14. J. H. Hildebrand and R. L. Scott, The Solubility of Non-electrolytes, Reinhold Publishing Corp., New York, N. Y., 3rd Edition, 1950.

15. P. Meares, Trans. Far. Soc. 47 699 (1951).

16. A. M. Saum, J. Polymer Sci. 42 57 (1960).

17. A. Ens and F. E. Murray, Can. J. Chem. 35 171 (1957).

18. R. G. Inskeep, J. M. Kelliher, P. E. McMahon and B. G. Somers, J. Chem. Phys. 28 1033 (1958).

19. R. M. Barrer, J. Phys. Chem. 61 179 (1957).

20. Lasoski, duPont Co., Private communication.

21. A. Kishimoto and K. Matsumoto, J. Phys. Chem. 63 1529 (1959).

22. S. Glasstone, K. J. Laidler and H. Eyring, The Theory of Rate Processes, McGraw Hill Book Co., New York, N. Y. 1941.

23. J. B. Wilkins and F. A. Long, Trans. Far. Soc. 53 1146 (1957).

24. G. J. van Amerongen, J. Applied Phys. 17 972 (1946).

25. G. Ya. Ryskin, Zhur. Tekh. Fiz. 25 458 (1954).

26. S. Sugden, J. Chem. Soc. 1924, 1177.

27. J. C. McGowan, Rec. Trav. Chem. 75 193 (1956).

28. J. Jeans, The Dynamical Theory of Gases, 4th Edition, Cambridge University Press, 1925; Dover Publications Inc., 1954.

29. C. W. Bunn, J. Polymer Sci. 16 323 (1955).

30. S. Lasoski, duPont Co., in publication.

31. A. S. Michaels and R. B. Parker Jr., J. Polymer Sci. 41 53 (1959).

32. C. Rogers, V. Stannett, and M. Szwarc, J. Phys. Chem. 63 1407 (1959).

33. A. W. Lawson, J. Chem. Phys. 32 131 (1960).

34. R. F. Clash, Jr. and L. M. Rynkiewicz, J. Ind. and Eng. Chem. 36 279 (1944).

35. S. Oya, Chem. High Polymers (Japan) 11 95 (1954), Chem. Abstr. 50 1444 (1956).

36. R. W. Keyes, J. Chem. Phys. 29 457 (1958).

37. W. J. Moore, Physical Chemistry, Prentice – Hall, Inc., New York, N. Y. 1950.

38. R. S. Spencer and G. D. Gilmore, J. Applied Phys. 20 502 (1949).

39. R. S. Spencer and R. F. Boyer, J. Applied Phys. 17 398 (1946).

40. W. W. Brandt, J. Phys. Chem. 63 1080 (1959).

41. P. Meares, Trans. Far. Soc. 53 101 (1959).

42. R. M. Barrer and G. Skirrow, J. Polymer Sci. 3 549 (1948).